

Quenching spin decoherence in diamond and single-molecule magnets

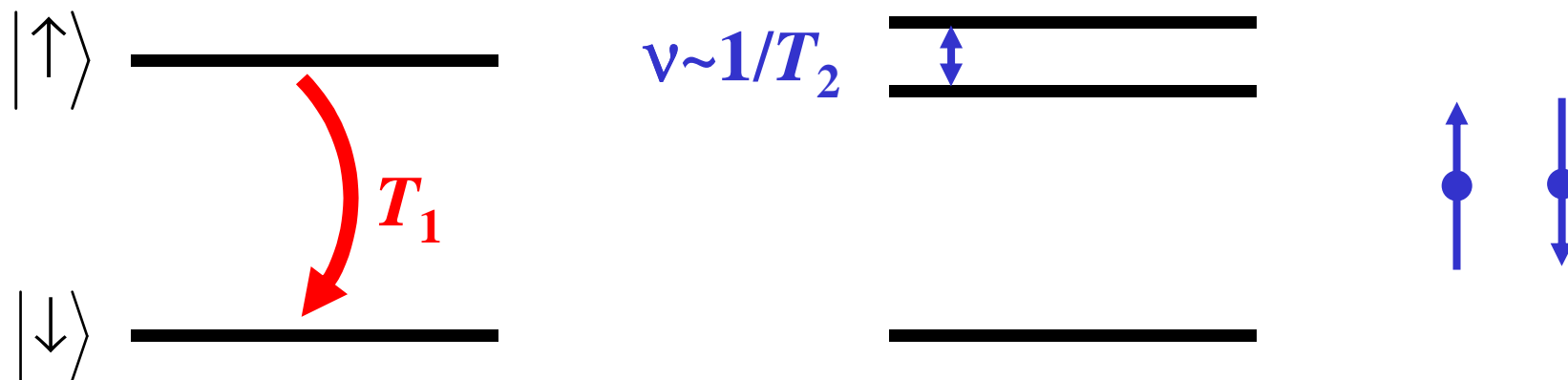
Susumu Takahashi

*Department of Physics and
Center for Terahertz Science and Technology
UC Santa Barbara*

Spin relaxation times T_1 and T_2

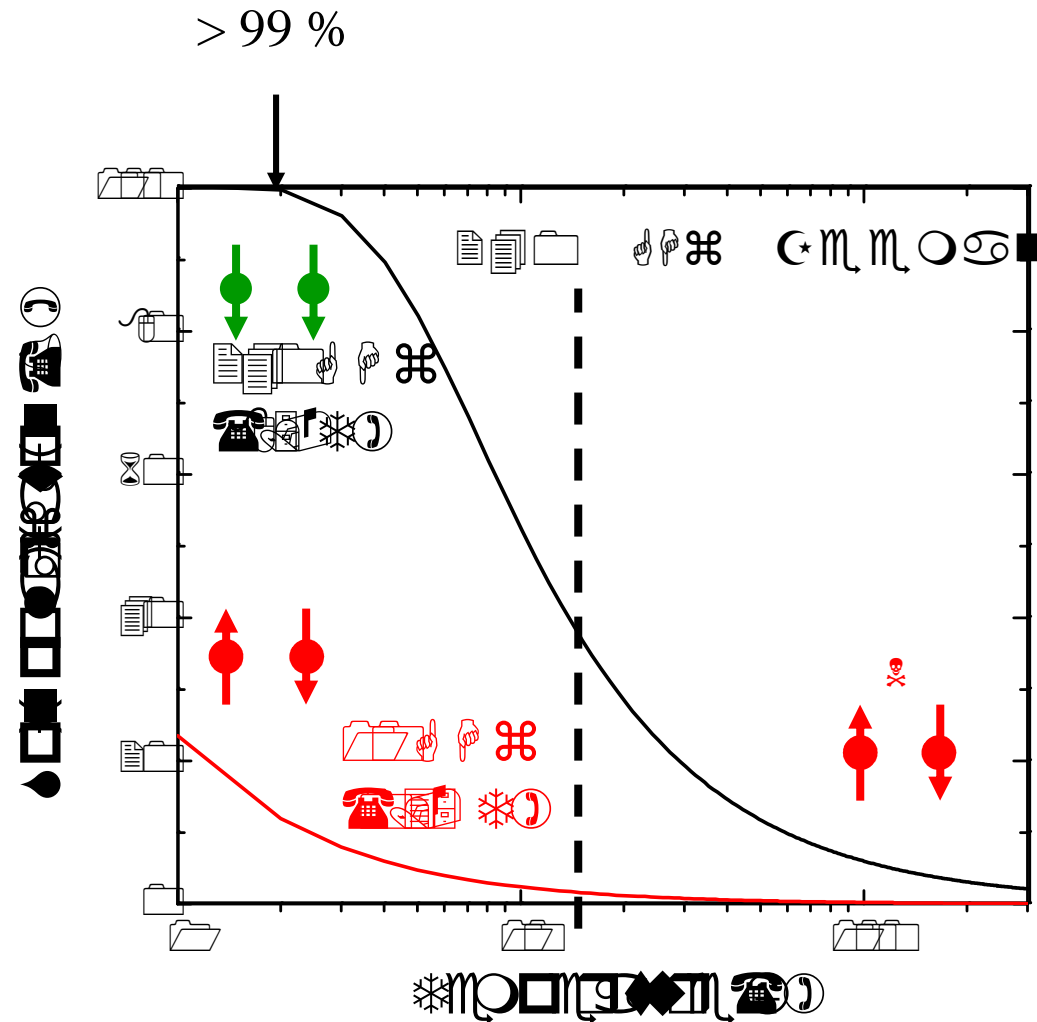


- T_1 : Relaxation from the excited state to the ground state. The total magnetization is changed (Energy-costing process). Typically caused by spin-lattice interactions.
- T_2 : Phase relaxation of spin precession. The total magnetization is NOT changed (Energy-conserving process). Typically caused by temporal spin-spin interactions (spin flip-flop).



High frequency EPR

- Spin polarization @ 2K
 - 240 GHz: 99.4 %
 - 10 GHz: 12 %
- Spin flip-flops are main decoherence source.
- Spin flip-flop rate \propto # of the up- and down-spin pair
- High polarization suppress spin decoherence

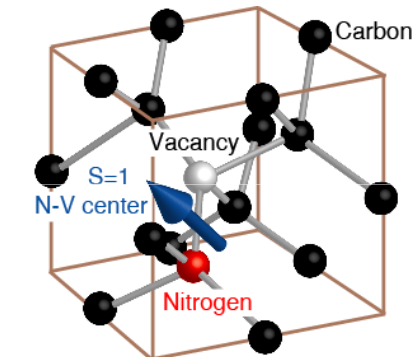


Outline

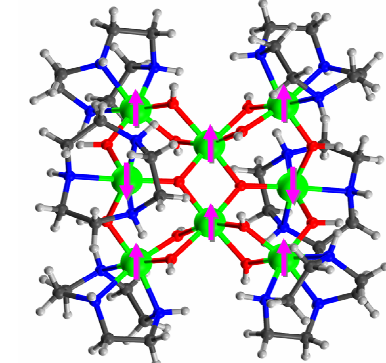


1. EPR with VDI source ($P \sim 30 \text{ mW}$)

- NV centers in diamond
- Single-molecule magnets

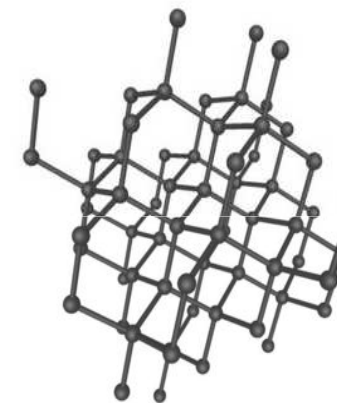


2. FEL-based pulsed EPR ($P \sim 1\text{kW}$)

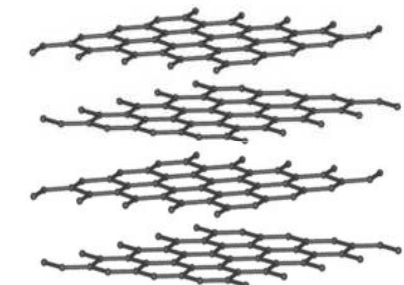


Diamond and impurities

- Hardest material
- Excellent thermal conductor
- A diamond is a crystal of tetrahedrally bonded carbon atoms.
- Diamond is classified by impurity contents.



Diamond



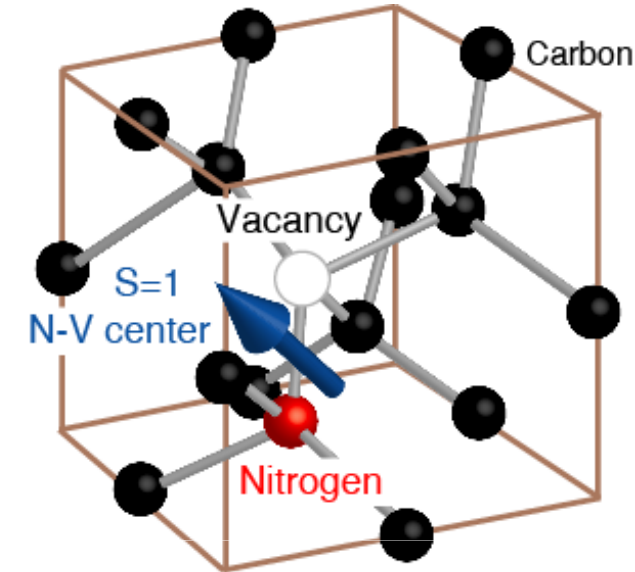
Graphite

Type	Ia	Ib	IIa	IIb
Natural abundance	~98 %	~0.1 %	1~2 %	~0 %
Nitrogen (ppm)	$\sim 2 \times 10^3$	$1 \sim 10^2$	~1	~1
Others (ppm)				~100 (B)
Color	Clear~Yellow	Yellow	Clear	Blue

NV centers in Diamond



- Quantum information processing
- Single photon source
- Single spin read-out
- Rapid spin polarization
- Long spin coherence time at room temperature
 - T. A. Kennedy *et al.*, *Appl. Phys. Lett.* **83**, 4190 (2003)
 - T. Gaebel *et al.*, *Nature Phys.* **2**, 408 (2006)

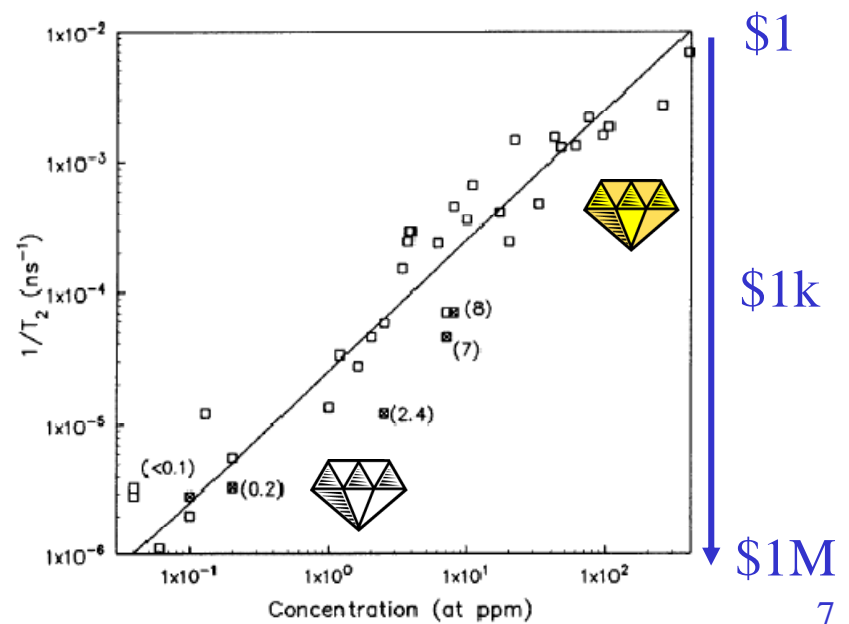
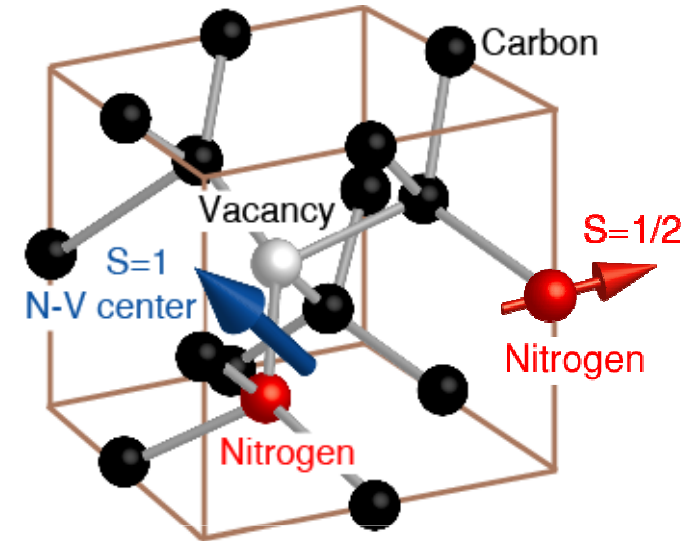


(D. D. Awschalom *et al.*,
Scientific American October 2007)

Decoherence of NV center



- N electron spin flip-flops
 - J. A. van Wyk *et al.*, *J. Phys. D: Appl. Phys.* **30**, 1790 (1997).
 - T. A. Kennedy *et al.*, *Appl. Phys. Lett.* **83**, 4190 (2003)
 - R. Hanson *et al.*, *Phys. Rev. B* **74**, 161203R (2006))
- No temperature dependence of T_2 @ 10 GHz
 - E. C. Reynamert *et. al.*, *J. Chem. Phys.* **109**, 8471 (1998))



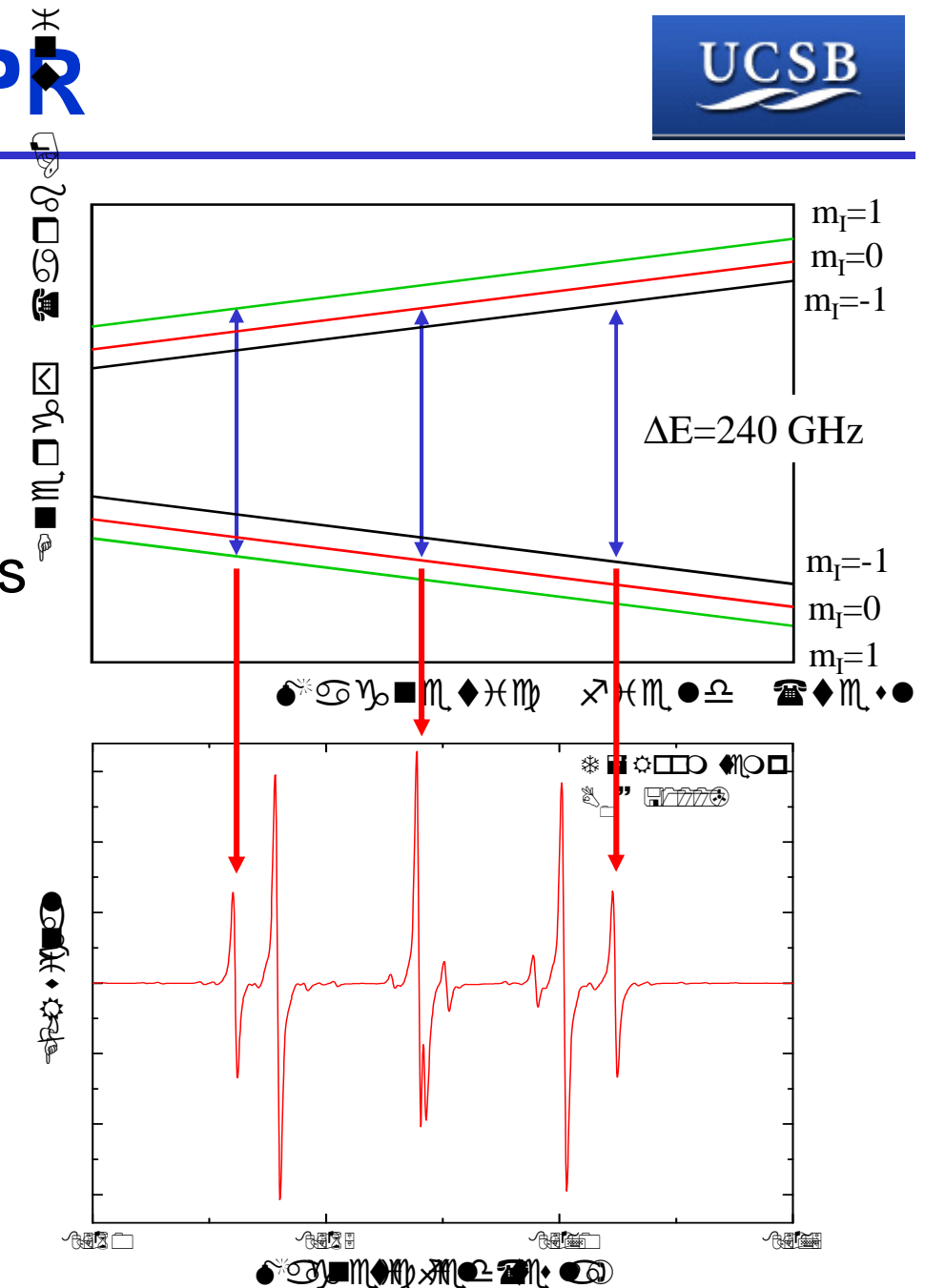
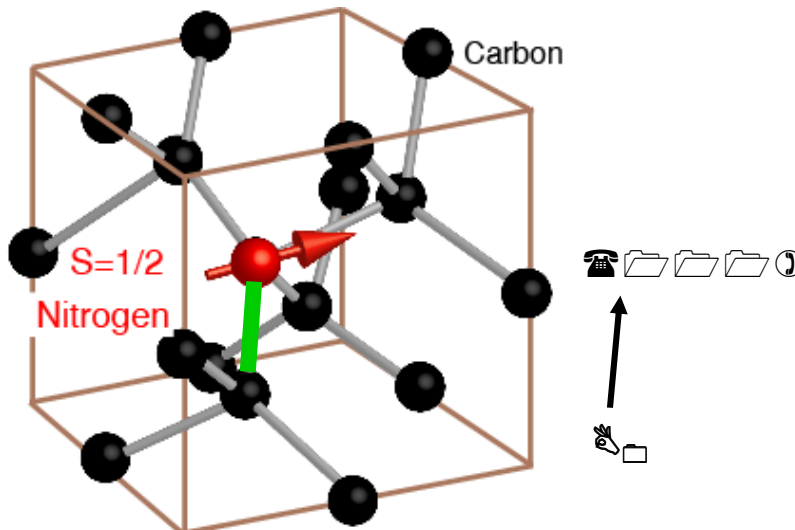
Continuous wave EPR



- N (single N) ($S=1/2$)

$$H_N = g\mu_B \mathbf{B} \cdot \mathbf{S} + \mathbf{S} \cdot \vec{\mathbf{A}} \cdot \mathbf{I}$$

- ^{14}N ($I=1$) hyperfine couplings



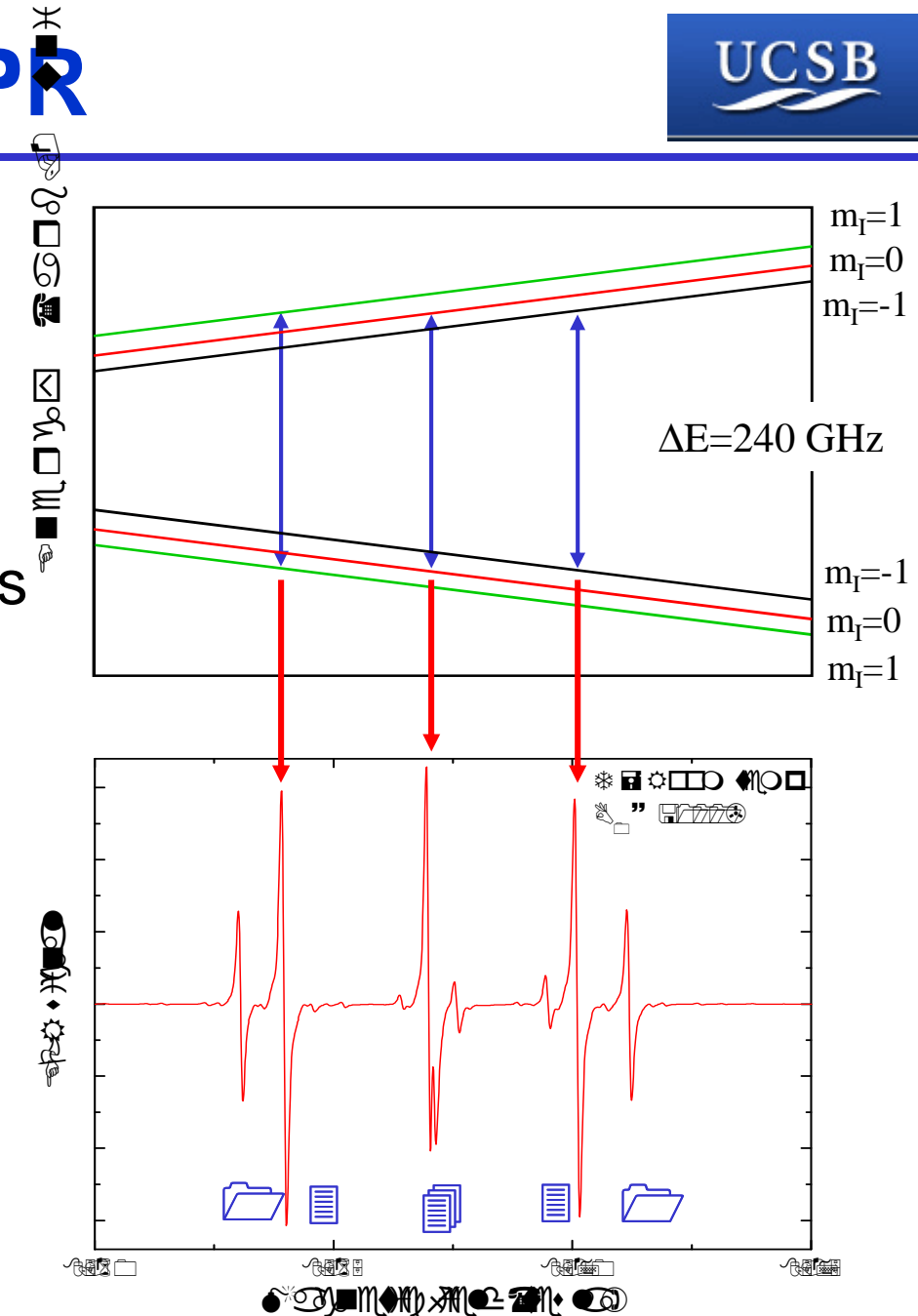
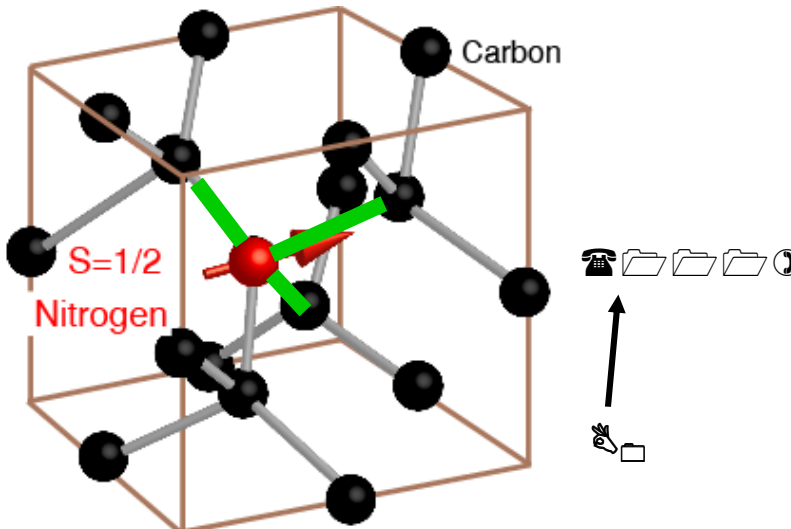
Continuous wave EPR



- N (single N) ($S=1/2$)

$$H_N = g\mu_B \mathbf{B} \cdot \mathbf{S} + \mathbf{S} \cdot \vec{\mathbf{A}} \cdot \mathbf{I}$$

- ^{14}N ($I=1$) hyperfine couplings
- Signal ratio=1:3:4:3:1

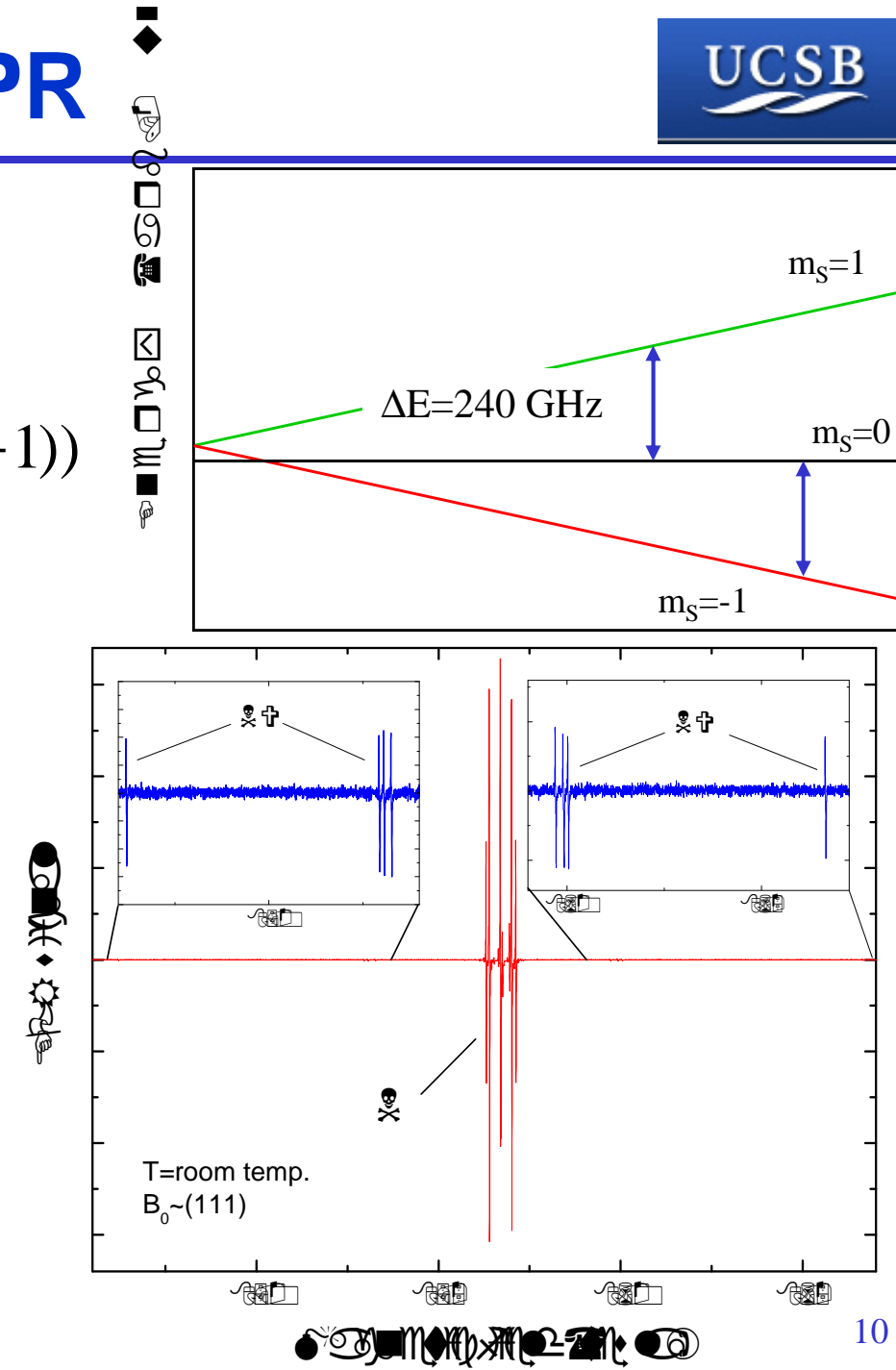
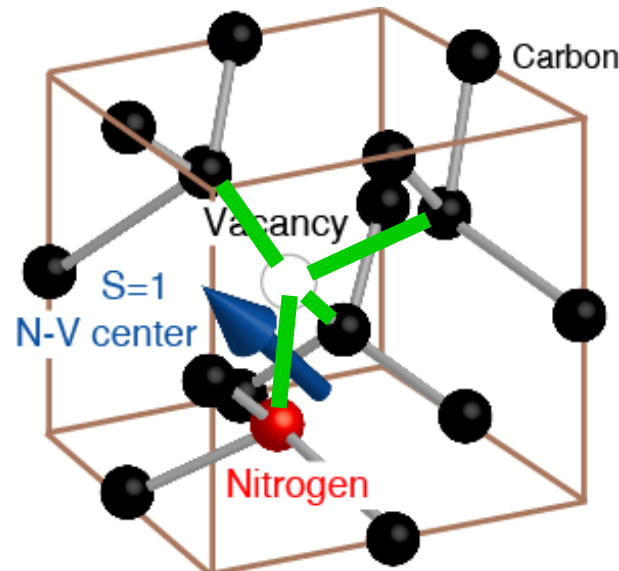


Continuous wave EPR

- NV center ($S=1$)

$$H_{NV} = g\mu_B \mathbf{B} \cdot \mathbf{S} + D(S_z^2 + 1/3S(S+1))$$

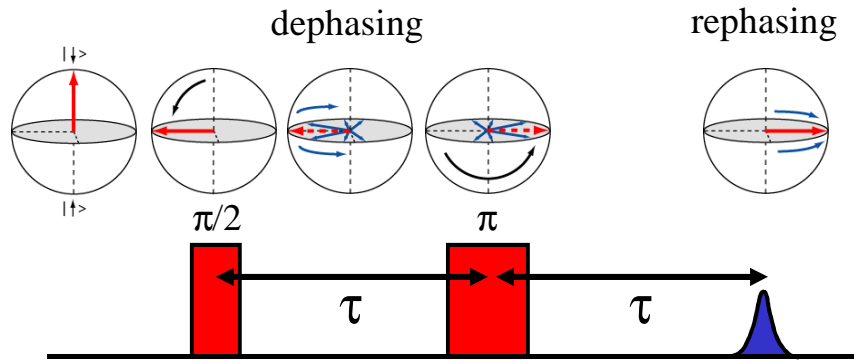
- Zero-field splittings



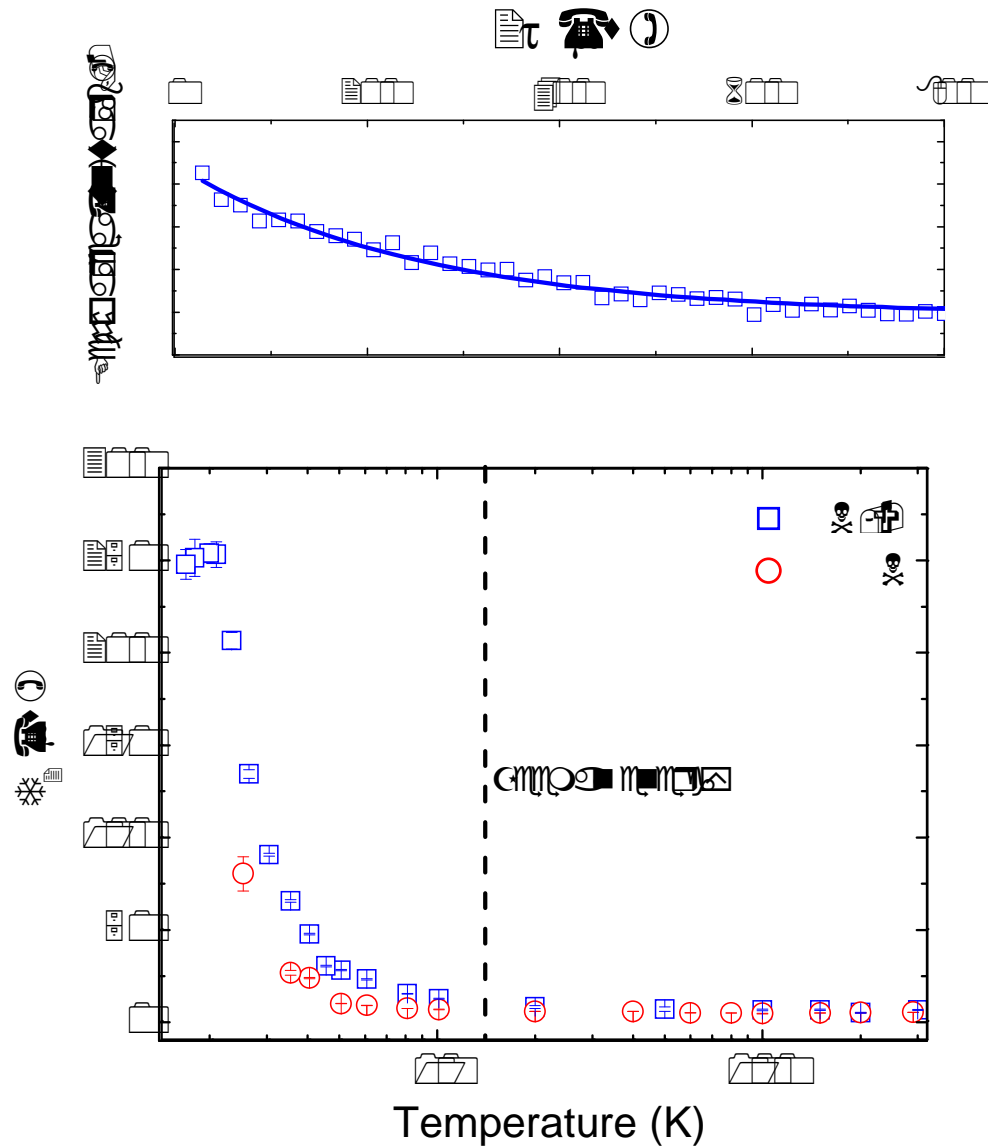
Temperature dependence of T_2



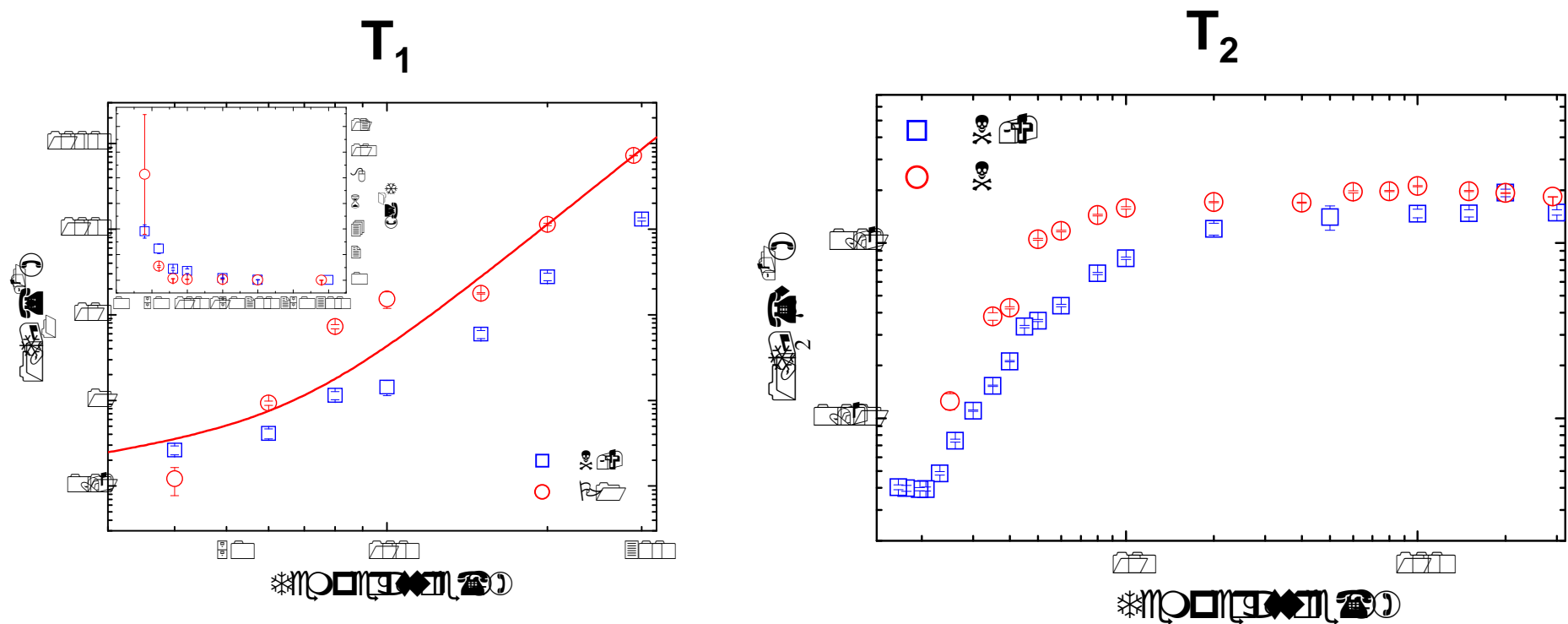
- Hahn echo sequence



- T_2 is obtained by a single exponential fit
- N-V:
 - $T > 11.5 \text{ K} : T_2 = 6.7 \mu\text{s} \rightarrow 8.3 \mu\text{s}$
 - $T < 2 \text{ K} : T_2 \sim 250 \mu\text{s}$
- N:
 - $T > 11.5 \text{ K} : T_2 = 5.5 \mu\text{s} \rightarrow 5.8 \mu\text{s}$
 - $T = 2.5 \text{ K} : T_2 \sim 80 \mu\text{s}$



Quenching spin bath decoherence



Quenching spin bath decoherence

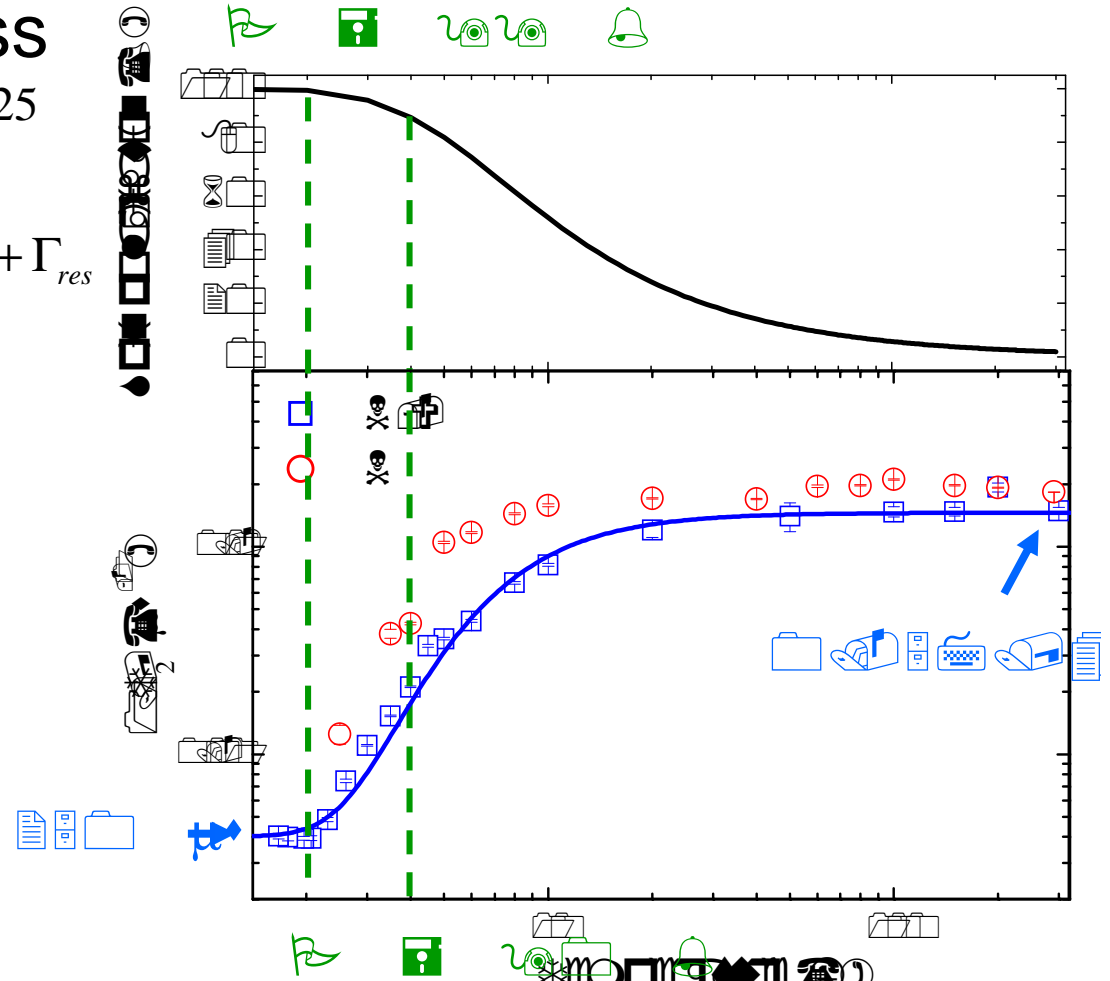


- N spin flip-flop process

(C. Kutter *et. al.*, *Phys. Rev. Lett.* **74**, 2925 (1995))

$$\frac{1}{T_2} = CP_{\uparrow}P_{\downarrow} + \Gamma_{res} = \frac{C}{(1+e^{T_{Ze}/T})(1+e^{-T_{Ze}/T})} + \Gamma_{res}$$

- 90 % for $10 \times T_2$
- 99 % for quenching
- C=0.57 MHz
- $1/\Gamma_{res} = 250 \mu s$



Dipole-dipole interaction



- $C=0.57 \text{ MHz}$

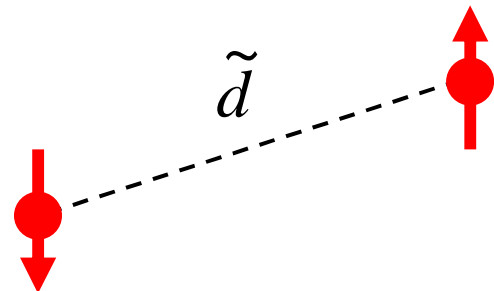
$$\frac{1}{T_2} \propto P_{\uparrow}P_{\downarrow} + \Gamma_{res} = \frac{C}{(1+e^{T_{Ze}/T})(1+e^{-T_{Ze}/T})} + \Gamma_{res}$$

- Dipole-dipole interaction energy

$$C = \frac{U_d}{h} \equiv \left\langle \frac{\mu_0}{4\pi} \frac{\mathbf{m}_1 \cdot \mathbf{m}_2 - 3(\mathbf{n} \cdot \mathbf{m}_1)(\mathbf{n} \cdot \mathbf{m}_2)}{\tilde{d}^3} \right\rangle / h$$

- $\tilde{d} = 2.8 \text{ nm} \rightarrow \text{N contents } \sim 25 \text{ ppm}$
- The sample crystal = 10 ~ 100 ppm
- **T₂-based distance measurement (Future plans)**

Average distance



^{13}C nuclear spin bath fluctuations



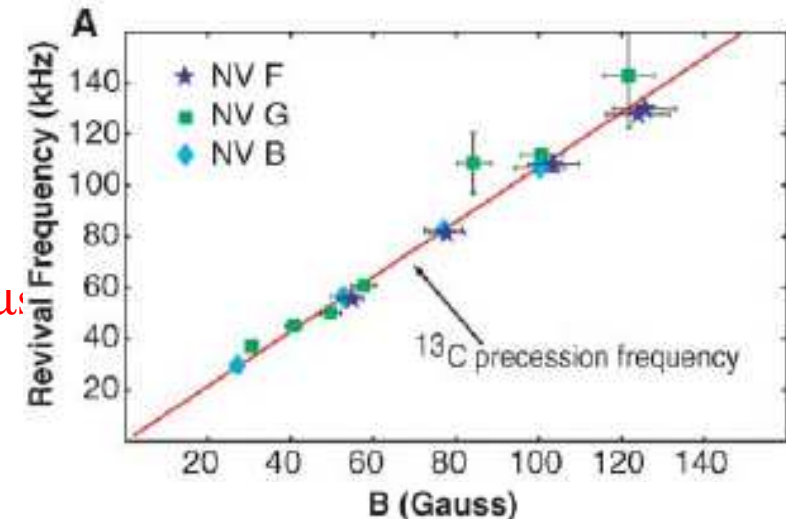
- $1/\Gamma_{\text{res}} = 250 \mu\text{s}$: Temperature independent relaxation rate

$$\frac{1}{T_2} \propto P_\uparrow P_\downarrow + \Gamma_{\text{res}} = \frac{C}{(1+e^{T_{\text{Ze}}/T})(1+e^{-T_{\text{Ze}}/T})} + \Gamma_{\text{res}}$$

$$1/\Gamma_{\text{res}} = 250 \mu\text{s}$$

- Decoherence time caused by ^{13}C nuclear spin flip-flop process

$$\frac{1}{T_2} = 0.49 \sqrt{\frac{\gamma_e}{\gamma_n}} \frac{\Delta\omega_{nn}}{[I(I+1)]^{1/4}} \sim \gamma_e^{1/2} \gamma_n^{3/2} N [I(I+1)]^{1/4}$$



L. Childress *et al.*, *Science* **314** 281 (2008)

where $\Delta\omega_{nn}$ is NMR linewidth, N is the number of nuclear per volume.

(I. M. Brown, Time domain electron spin resonance, p195, Wiley (1979).

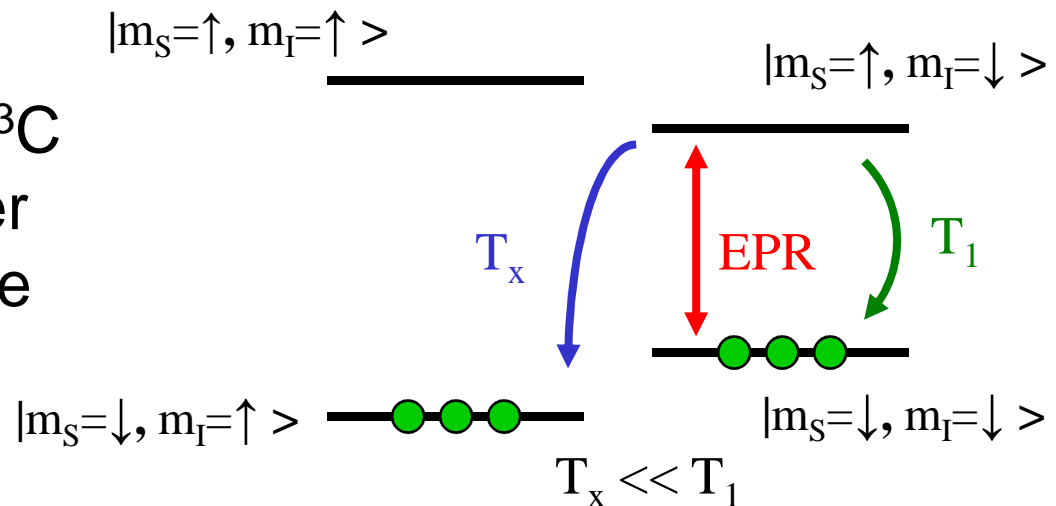
A. Schweiger and G. Jeschke, Oxford university press (2001)).

- $T_2 \sim 380 \mu\text{s}$ for ^{13}C nuclear spin bath fluctuations

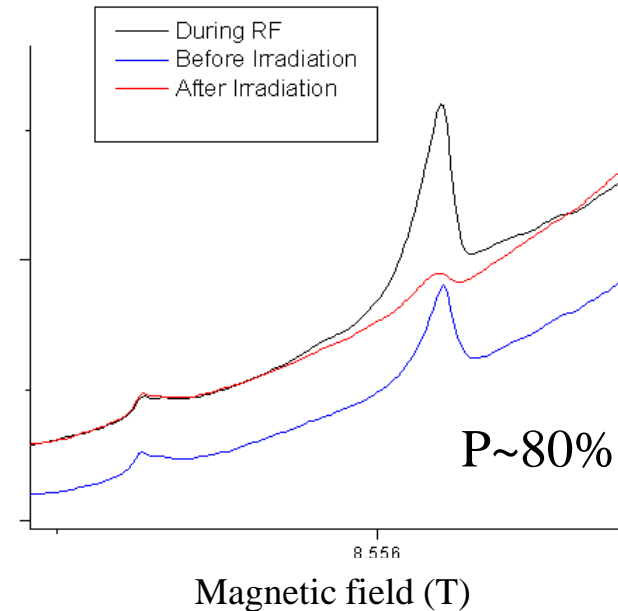
S. Takahashi *et al.*, *Phys. Rev. Lett.* **101**, 047601 (2008)

Polarizing ^{13}C nuclear spins

- Suppress fluctuations of ^{13}C nuclear spin bath to further increase spin decoherence time.



- Dynamic nuclear polarization (DNP) may be able to polarize the nuclear spin bath.
- High polarization of N electron spins is a key.



Summary - diamond

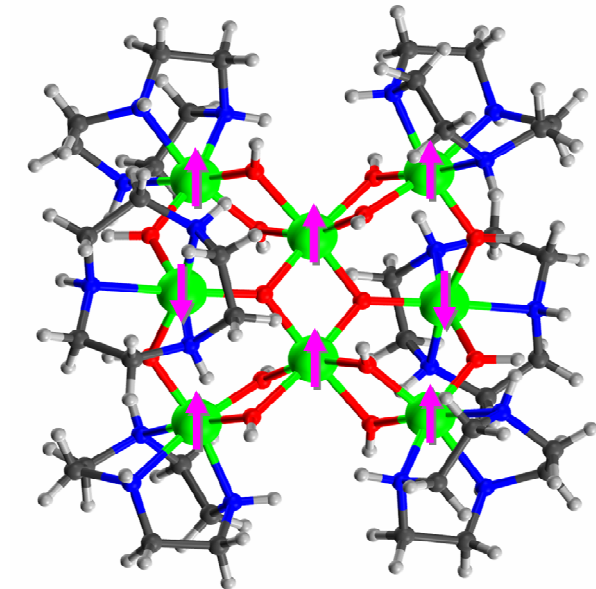


- We demonstrated that spin decoherence of electron spin bath can be quenched by high-fields and low-temperatures.
- We can access a nuclear spin bath decoherence.
- Temperature dependence of T_2 is potentially useful for distance measurements.

Outline

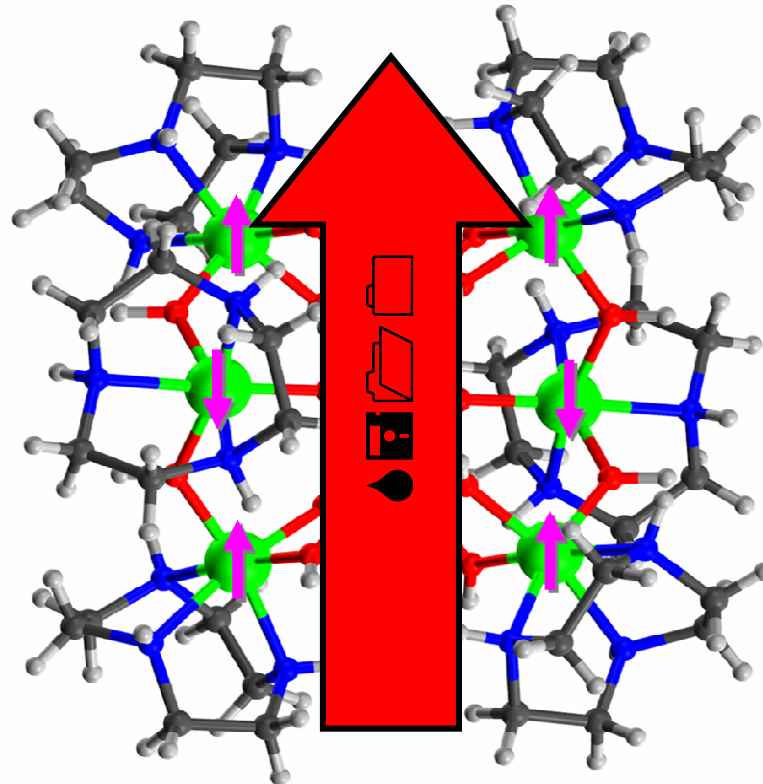
1. EPR with VDI source (P~30 mW)

- NV centers in diamond
- **Single-molecule magnets**



2. FEL-based pulsed EPR (P~1kW)

Single-molecule magnets



● : Fe^{3+} ($S=5/2$)

● : O ● : N

● : C ● : H

K. Wieghardt *et al.*, G. Angew. Chem., Int. Ed. Engl. 23, 77 (1984).

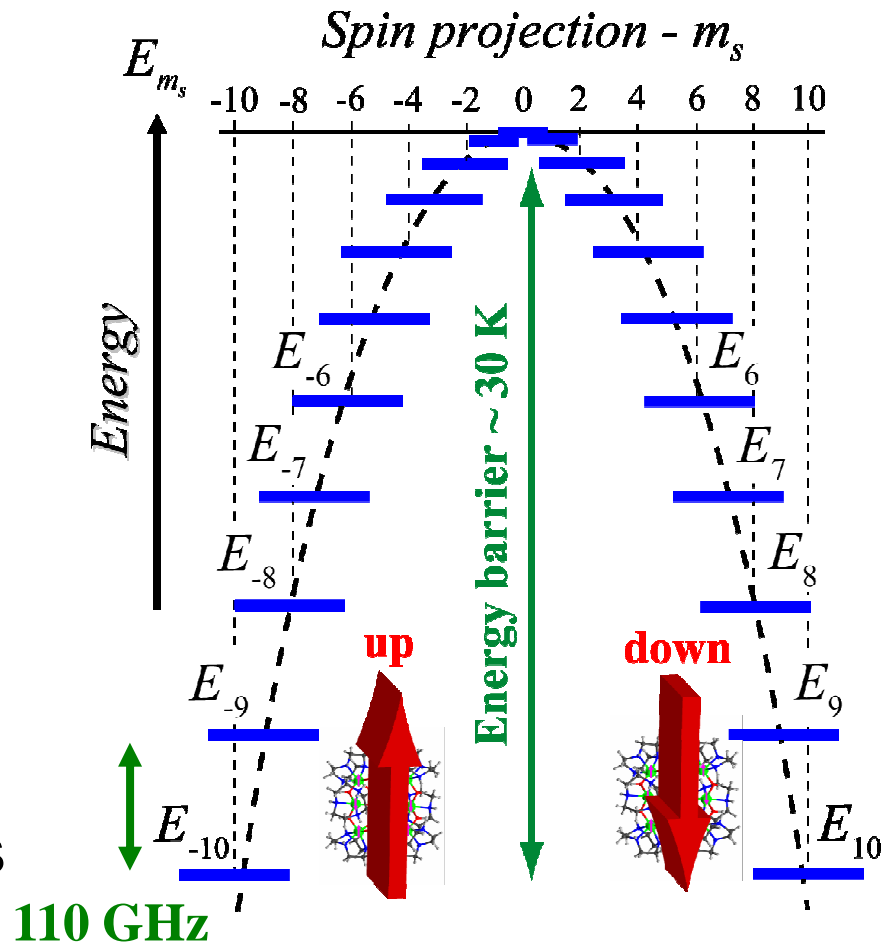


- High-spin molecular magnets made by metal-ion clusters
- Chemically fabricated quantum dots
- $S=10$ Fe_8 SMM
Total spin = $(6-2)\times 5/2=10$
- Weakly interacts with each other, ensemble properties express themselves as a pseudo-giant single spin.

Energy barrier



- Anisotropy due to crystal field.
- For Fe_8 , uniaxial anisotropy
- Energy barrier = $D\mathbf{S}_z^2 \sim 30\text{K}$
- Superparamagnets at high T
- Magnetic relaxation becomes very slow at low T, so becomes magnets.



Quantum \leftrightarrow Classical



macroscale



nanoscale

permanent
magnets

micron
particles

nanoparticles

clusters

Molecular
clusters

Individual
spins

100 nm

10 nm

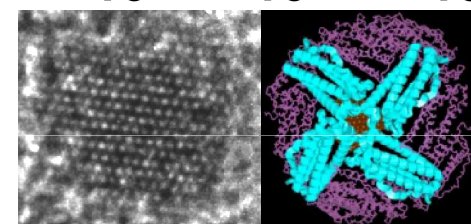
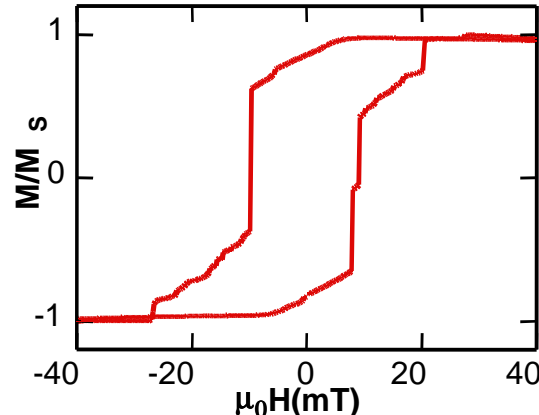
1 nm

$$S = 10^{23} \quad 10^{10} \quad 10^8 \quad 10^6 \quad 10^5 \quad 10^4 \quad 10^3 \quad 10^2 \quad 10 \quad 1$$



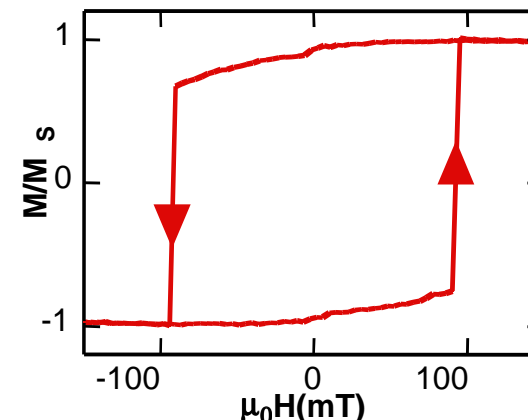
multi - domain

nucleation, propagation and
annihilation of domain walls



single - domain

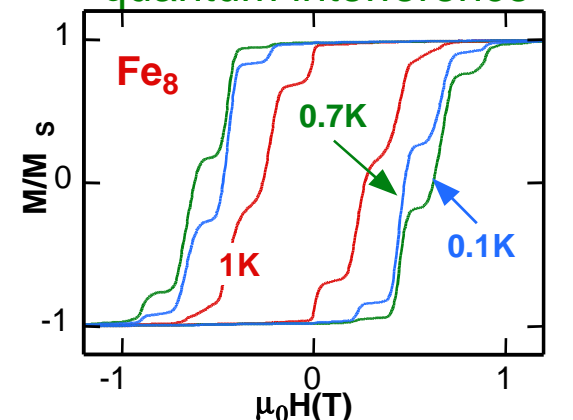
uniform rotation



Ferritin

magnetic moment

quantum tunneling,
quantum interference



cw EPR – angle dependence

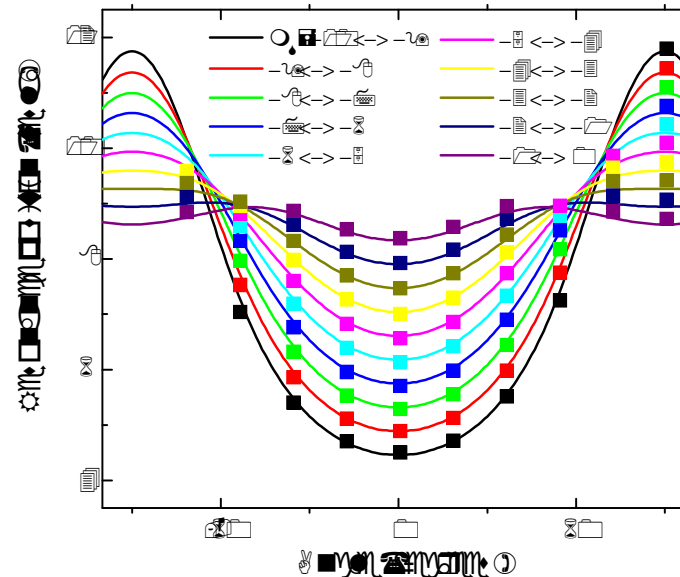
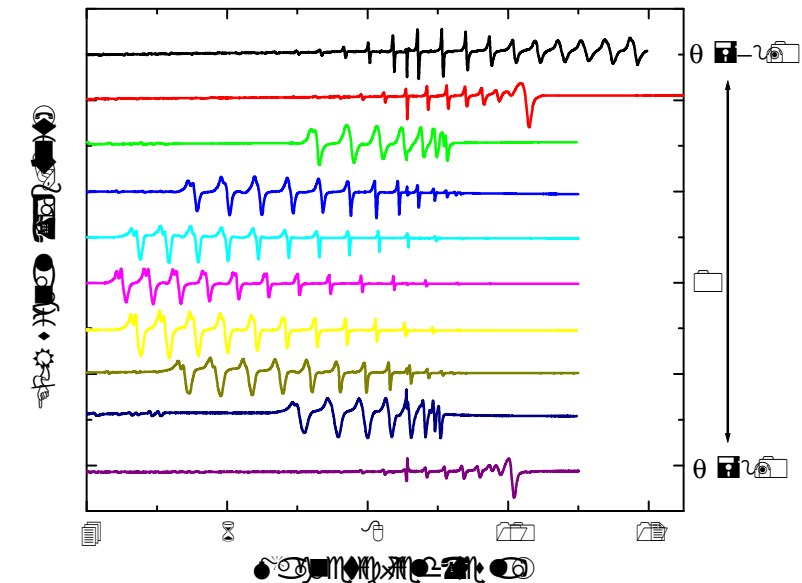
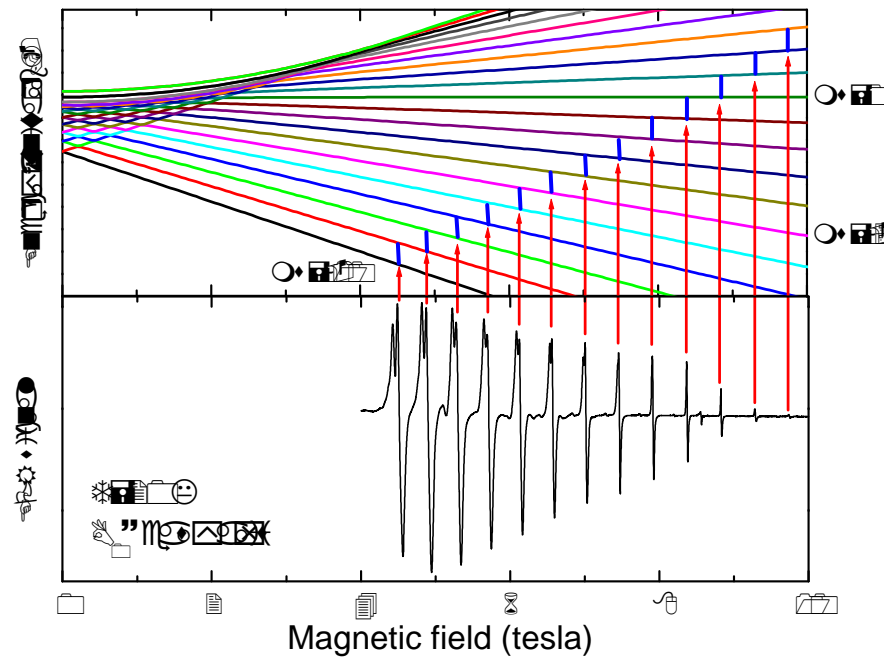


- Spin Hamiltonian for individual Fe_8 SMM

$$H = \mu_B g \mathbf{S} \cdot \mathbf{B}_0 + D S_z^2 + E (S_x^2 - S_y^2)$$

$g=2.00$, $D=-6.15$ GHz, $E=1.14$ GHz

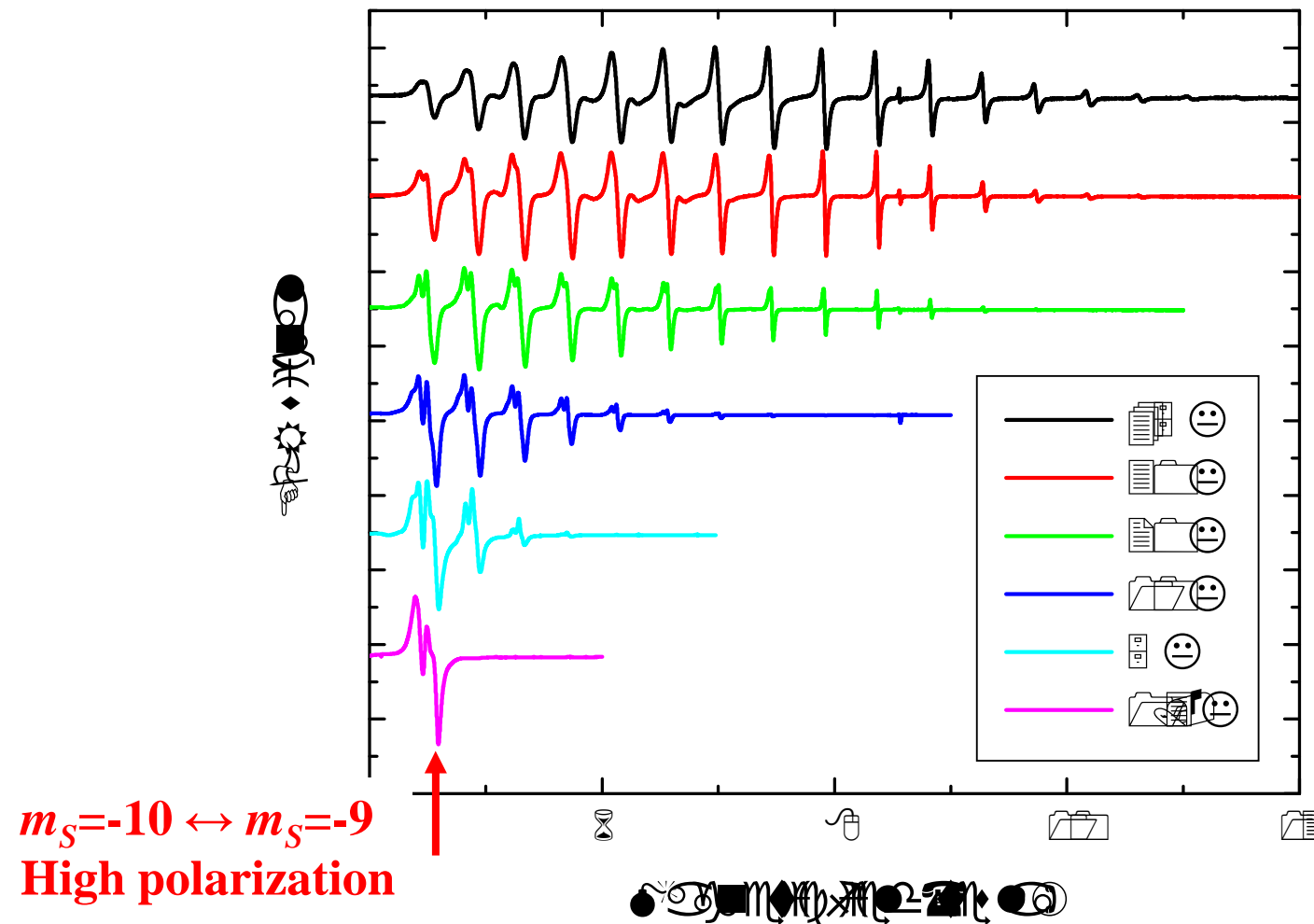
- A single crystal was rotated as function of a magnetic field.



cw EPR – temperature dependence



- $B \sim$ easy axis
- Indicates the ground state peak at 4.6 T.



Spin decoherence of SMMs

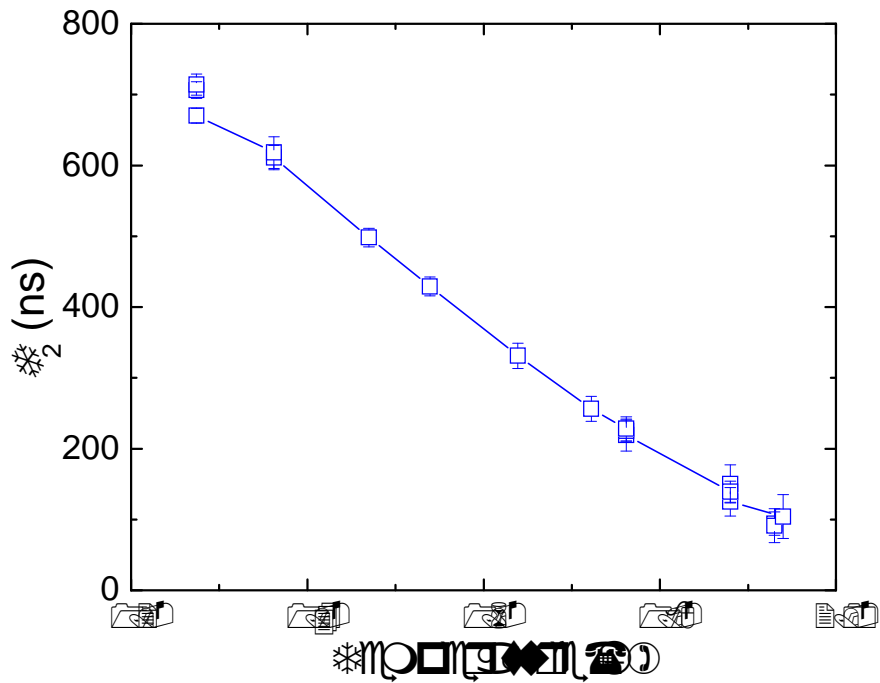
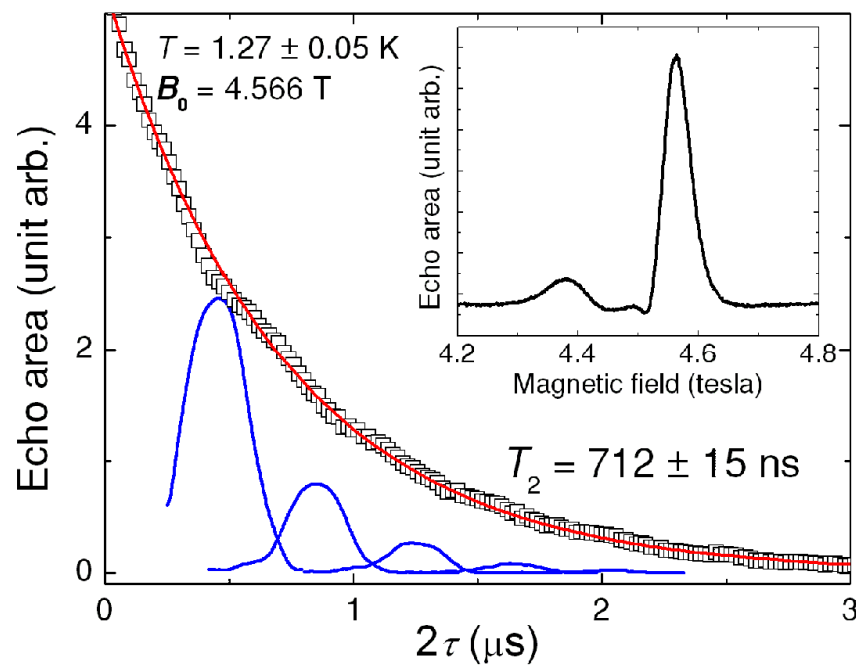
- No publication of spin echo from single-crystal SMMs.
- T_2 will be very short because of strong fluctuations of SMM spin bath.
- There are some observations of spin echo from highly diluted molecular magnets.
 - C. Schlegel *et al.*, *Phys. Rev. Lett.* **101**, 147203 (2008).
 - A. Ardavan *et al.*, *Phys. Rev. Lett.* **98**, 057201 (2007).
 - S. Bertaina *et al.*, *Nature* **453**, 203 (2008).
- Fluctuations of electron spin bath can also be reduced by polarizing the spin bath.

First spin echo measurement



- Strong temperature dependence indicates electron spin bath fluctuations.
- $T_1 \sim 1 \text{ ms} \gg T_2$

T_2 measurement



S=10 Fe₈ spin bath fluctuations

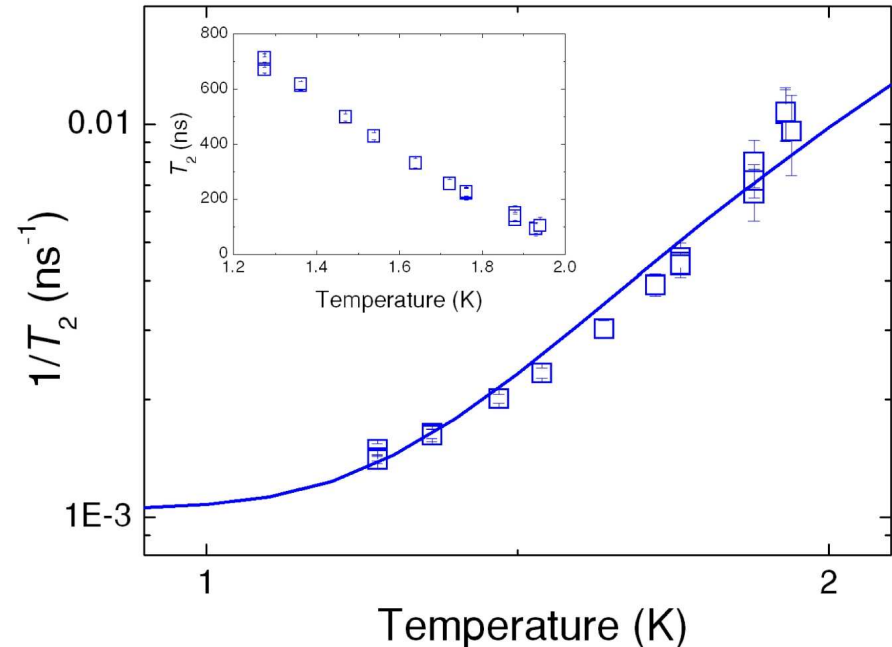
- S=10 spin flip-flop process:

$$\frac{1}{T_2} = A \sum_{m_S=-10}^9 W(m_S) P_{m_S} P_{m_S+1} + \Gamma_{res}$$

$$P_{m_S} = \frac{e^{-\beta E(m_S)}}{Z}$$

$$W(m_S) = \left| \langle m_S + 1, m_S | S_1^+ S_2^- | m_S, m_S + 1 \rangle \right|^2 + \left| \langle m_S, m_S + 1 | S_1^- S_2^+ | m_S + 1, m_S \rangle \right|^2$$

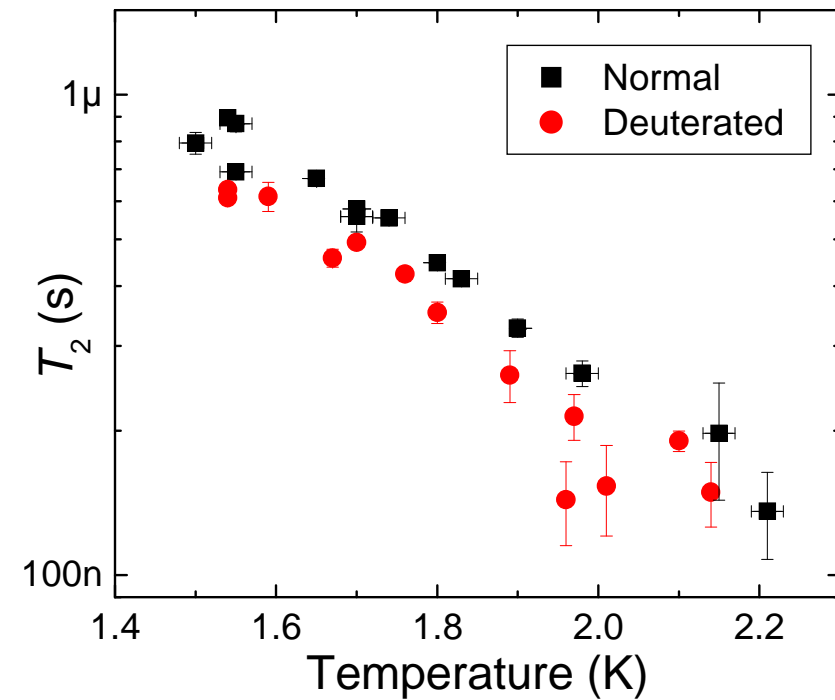
- Spin decoherence is significantly suppressed by spin polarization.
- Γ_{res} may be caused by couplings to nuclear moments (Proton & ⁵⁷Fe) and phonon.



No ^1H spin bath decoherence?

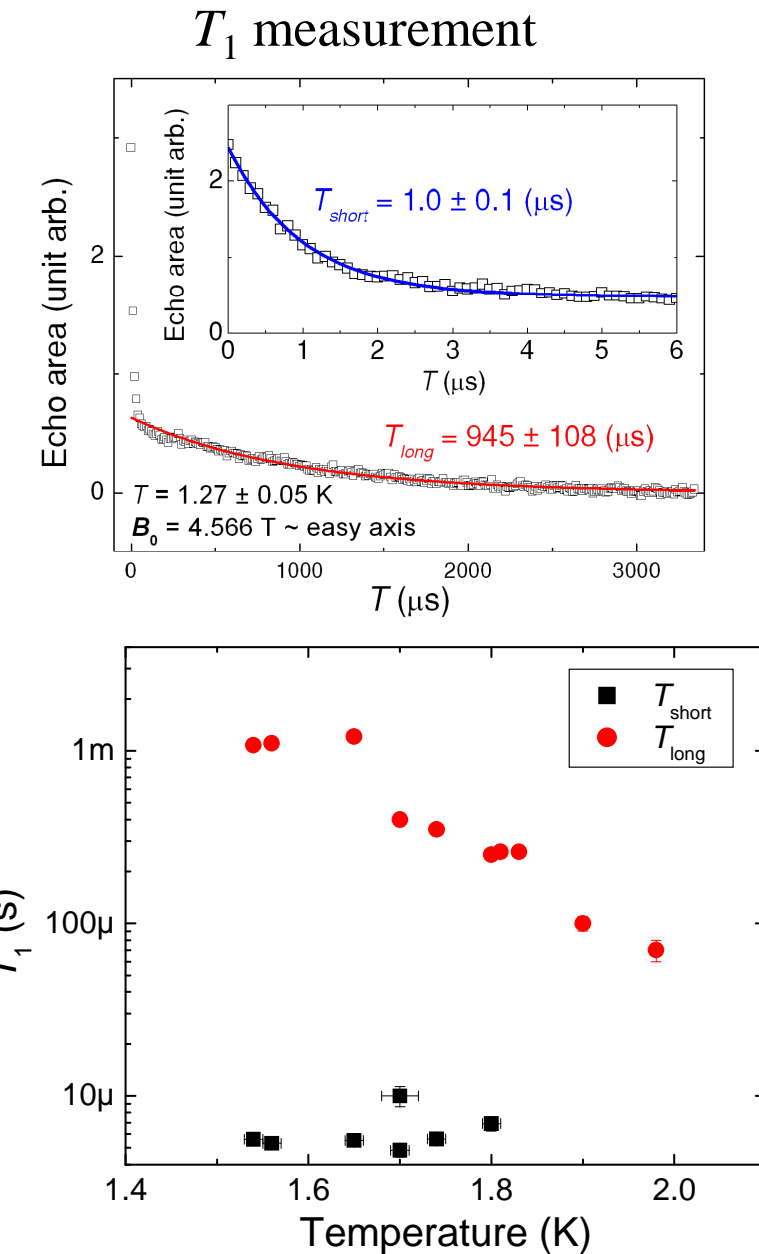
- Deuterated Fe_8 SMM was recently studied.
- Deuterium has much smaller magnetic moments than Hydrogen.
- Temperature dependence of T_2 is about same.
- A theory predicts that phonon decoherence $>>$ nuclear decoherence.

A. Morello *et al.*, *Phys. Rev. Lett.* **97**, 207206 (2006)



T_1 relaxation time

- Two decay curves have been measured.
- T_{long} : temperature-dependent (T_1)
Similar relaxation is reported by K. Petukhov *et al.*, Phys. Rev. B **75**, 064408 (2007).
- T_{short} : temperature-independent (Spectral diffusion?)
- Other T_1 measurements
 ~2 us: S. Bahr *et al.*, Phys. Rev. Lett. **99**, 147205 (2007)
 ~ 40 ns: M. Bal *et al.*, Europhys. Lett. **71**, 110 (2008)



S. Takahashi *et al.*, unpublished.

Summary – SMMs

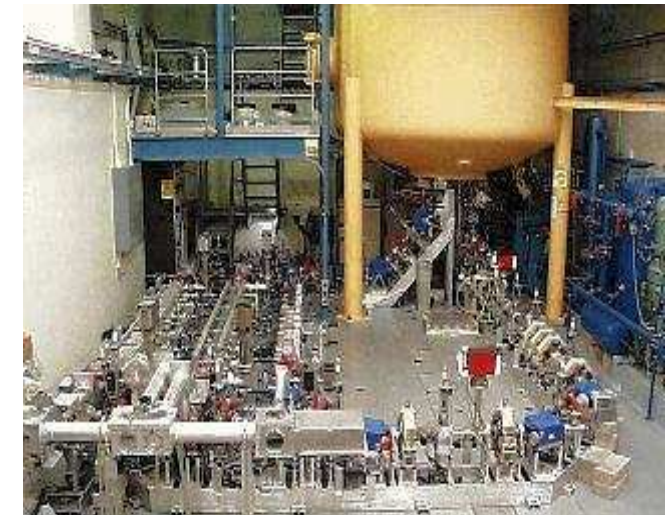
- We observed spin echo in Fe_8 single crystals for the first time by suppressing spin decoherence.
- Low temperature T_2 is limited $\sim 1\mu\text{s}$.
- We are investigating the other decoherence sources and the origin of T_1 .

Outline



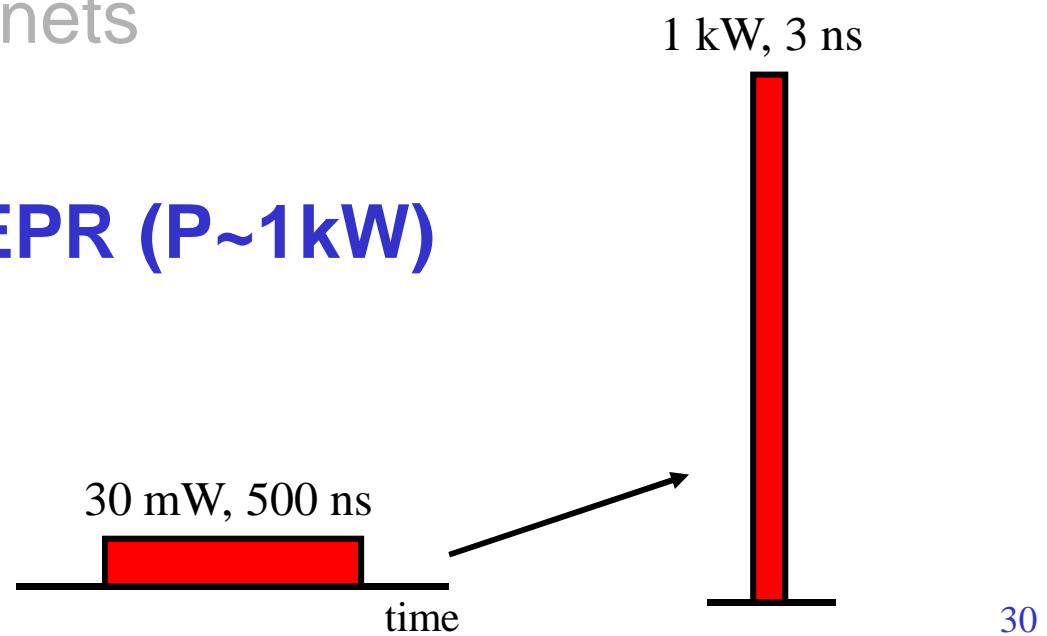
1. EPR with VDI source ($P \sim 30 \text{ mW}$)

- NV centers in diamond
- Single-molecule magnets



2. FEL-based pulsed EPR ($P \sim 1 \text{ kW}$)

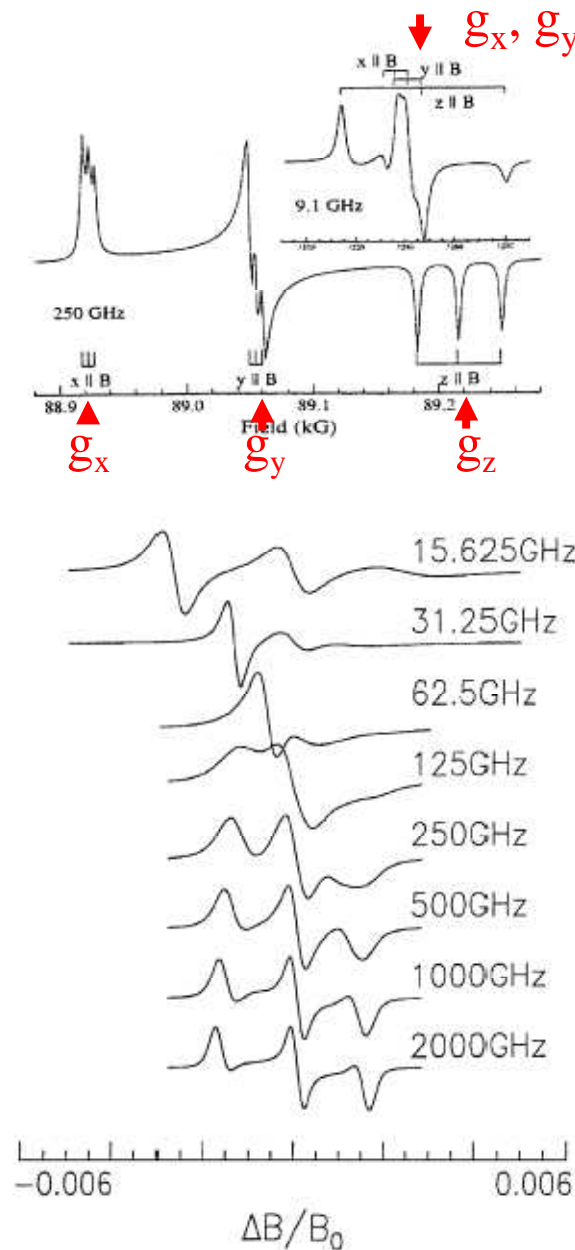
Tip angle of spins: $\alpha \propto B_{MW} \cdot t$



High-frequency EPR

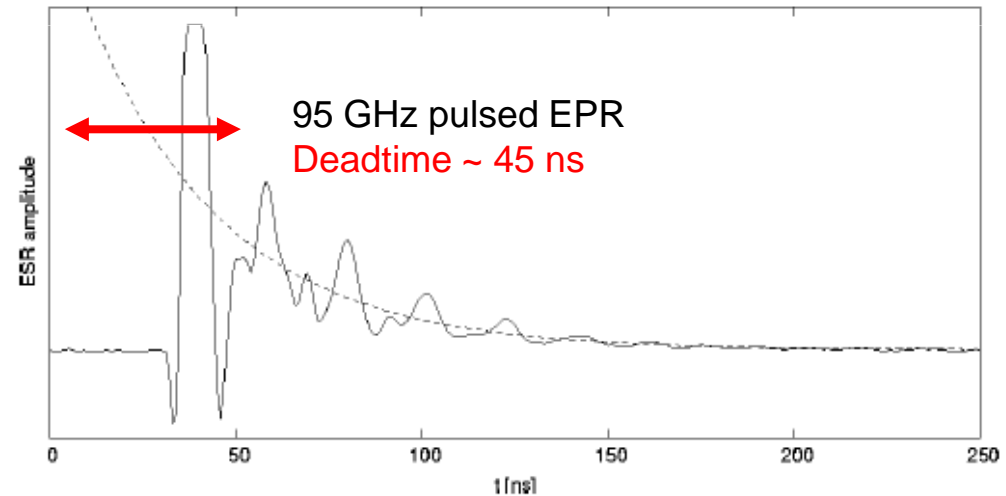
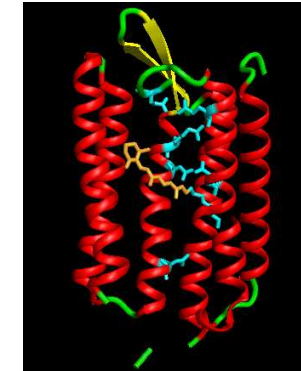


- Finer spectral resolution
- Less motional averaging
- Higher spin polarization
- Low-power/High-frequency pulsed EPR spectrometers (>150 GHz)
 - NHMFL (120, 240, 336 GHz)
 - Leiden (275 GHz)
 - Frankfurt (180 GHz)
 - Freie U. Berlin (360 GHz)
 - UCSB (240 GHz)
- High-power/High-frequency ($P \sim 100 - 1\text{ kW}$)
- Better time resolution



High-power pulsed EPR

- Short spin relaxation time (T_1 and T_2), e.g. SMMs & proteins in aqueous solution.
- Fast structure change, e.g. “film” proteins in action
- 10 GHz and 35 GHz pulsed EPR systems with 100 ns time resolution
- High frequency EPR for better time resolution
 - Shorter deadtime (\bullet Q/ω)
- A few 95 GHz systems.
 - Freed group (Cornell)
 - Smith group (St. Andrews, UK)
- No commercial high power THz source.
- UCSB FEL covers up to 4.7 THz (1.26 THz = 45 tesla for g=2 EPR)

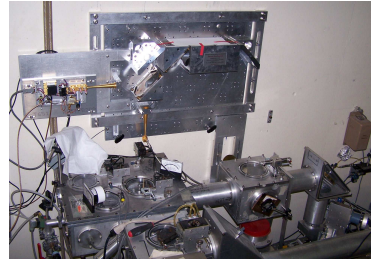


W. Haufbauer *et al.*, *Rev. Sci. Instrum.* **75**, 1202 (2004)

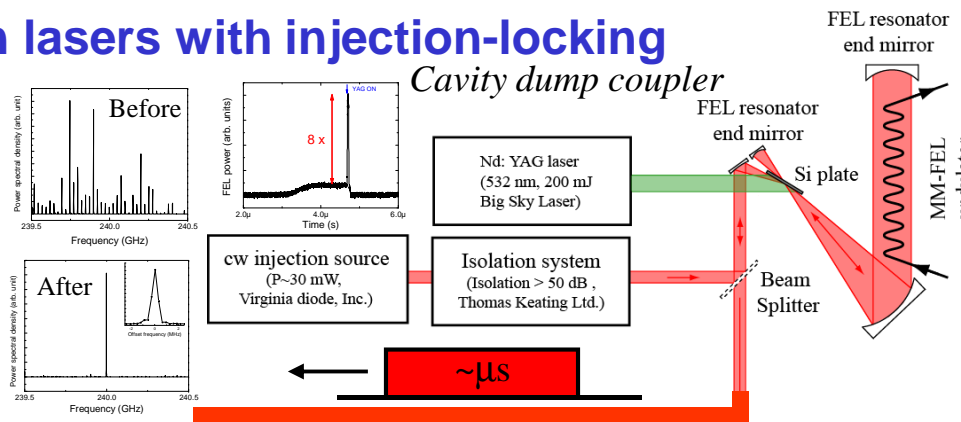
Setup overview



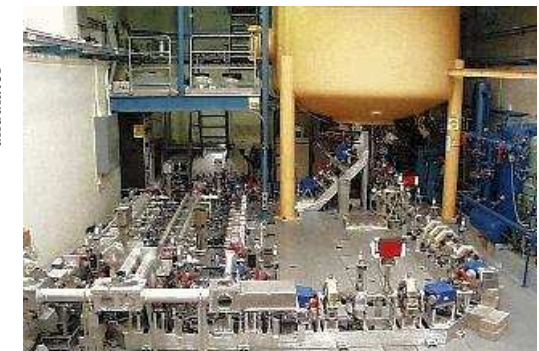
1. Free-electron lasers with injection-locking



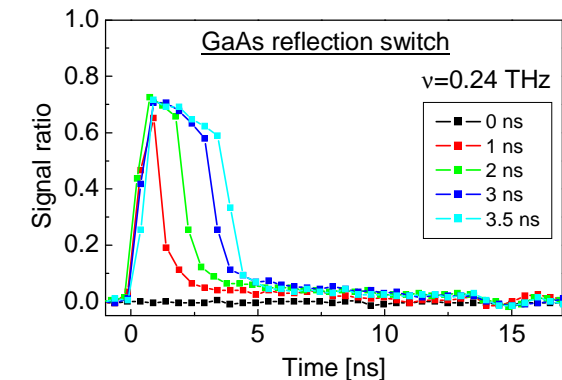
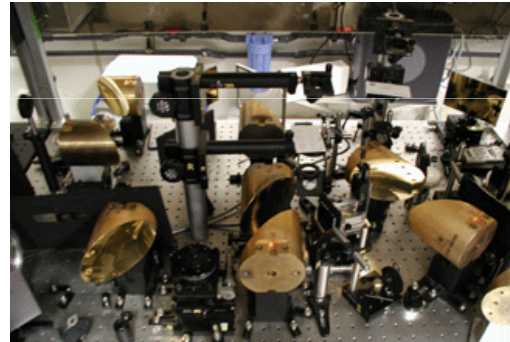
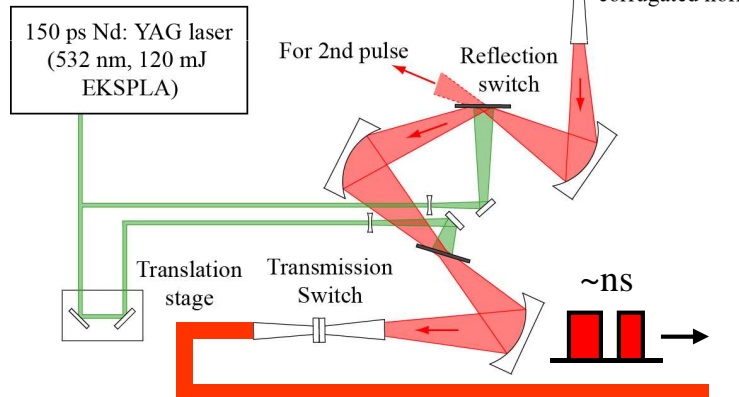
Injection-locking system



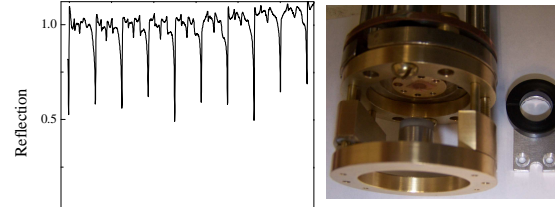
UCSB FELs (120 GHz – 4.7 THz)



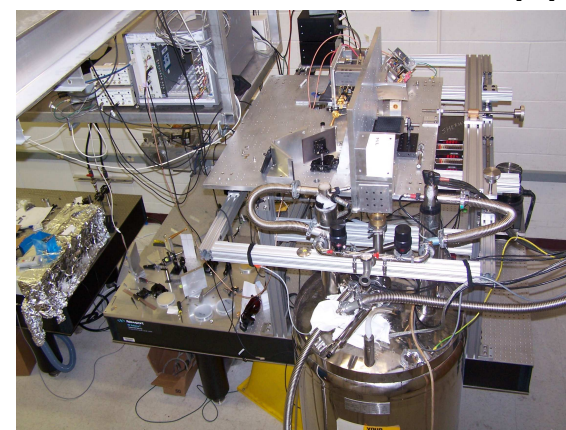
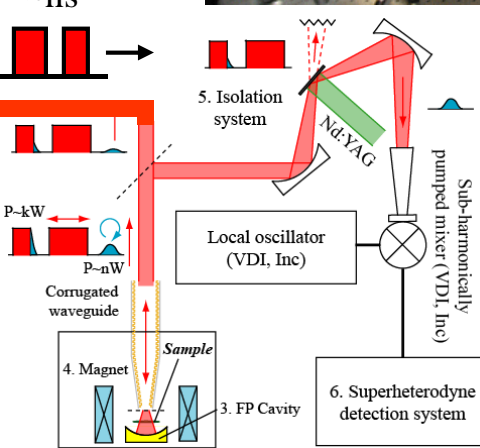
2. Pulse Slicer



3. EPR spectrometer



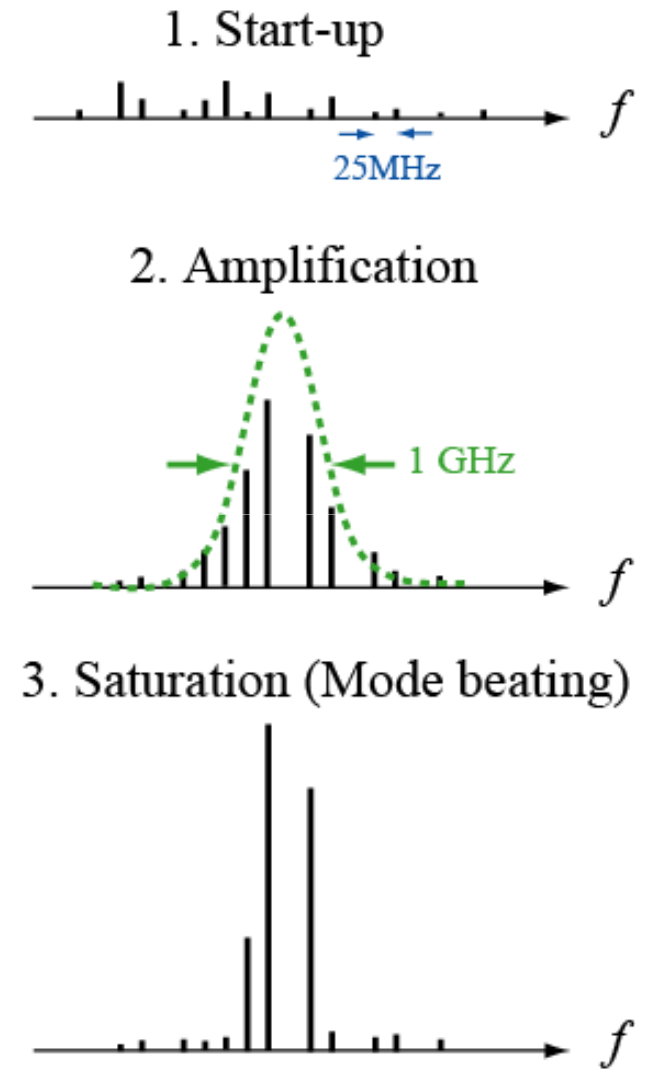
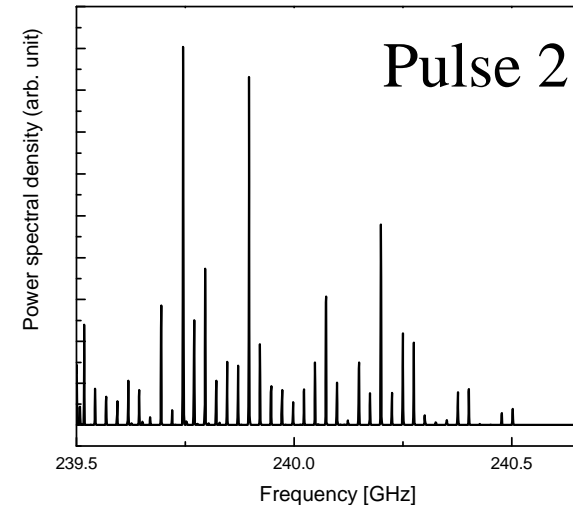
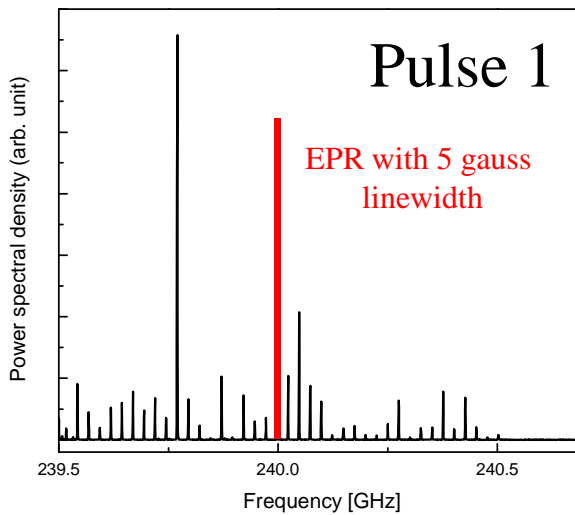
Fabry-Perot cavity



FEL - multimode radiation



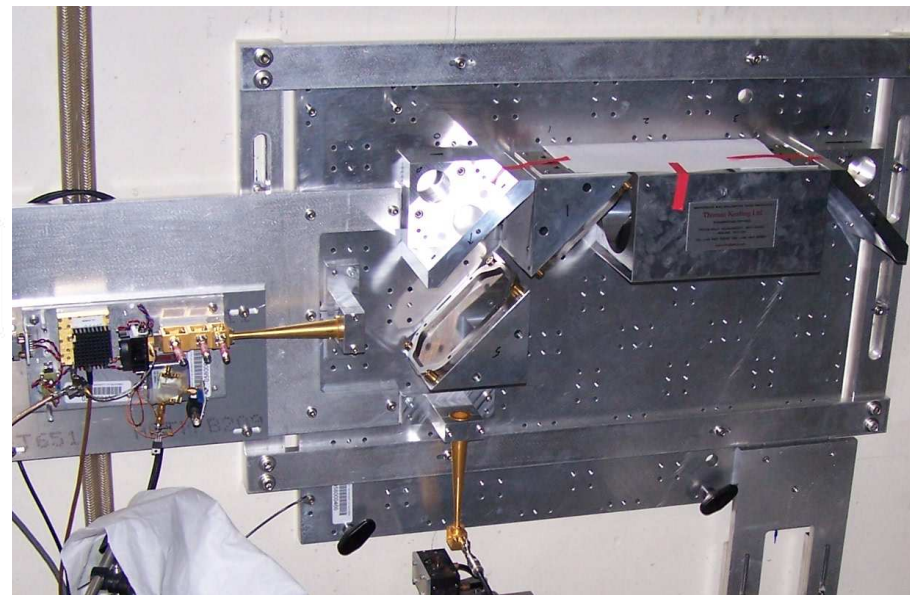
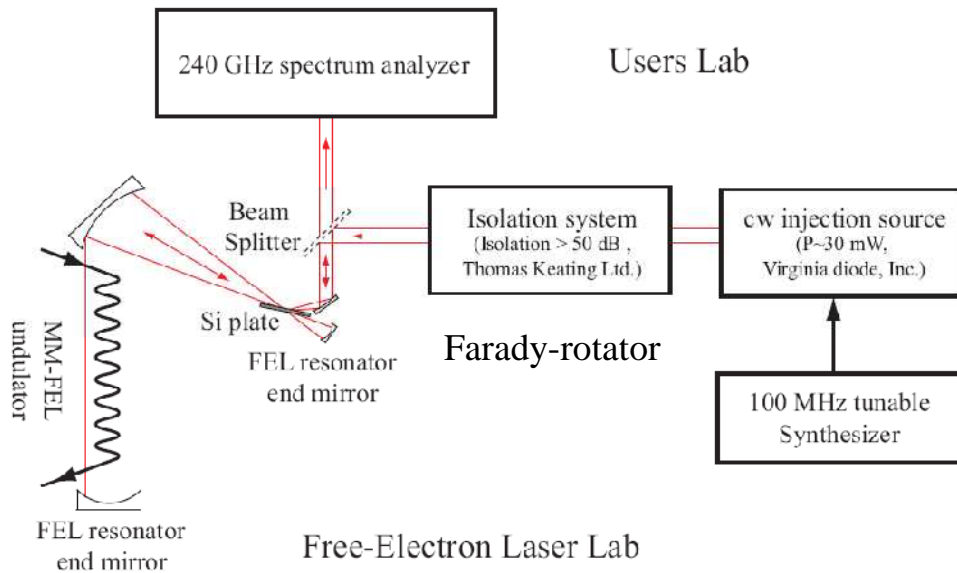
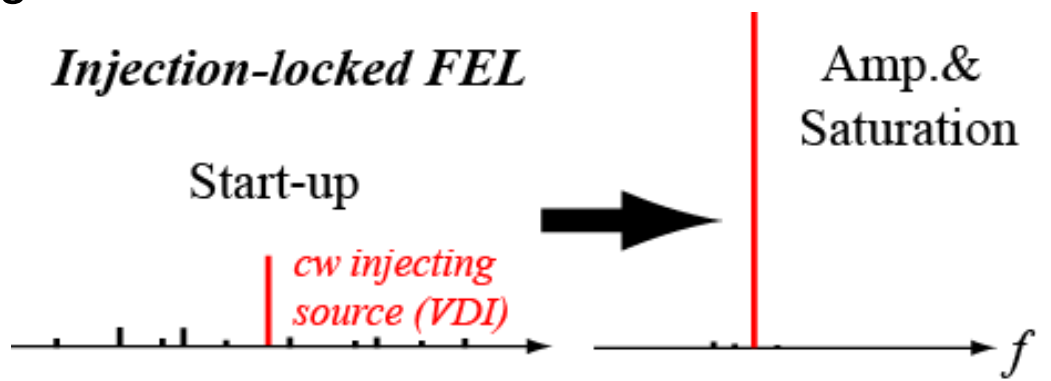
- We built 240 GHz spectrum analyzer to observe FEL spectrum.
- UCSB FEL employs a 6 m (20feet) long Fabry-Perot cavity (25 MHz mode spacing) in the undulator.
- Radiation modes of the FEL depend on stochastic start-up process and FEL gain bandwidth ~ 1 GHz.
- Multimode lasing and pulse-to-pulse frequency



Injection-locking

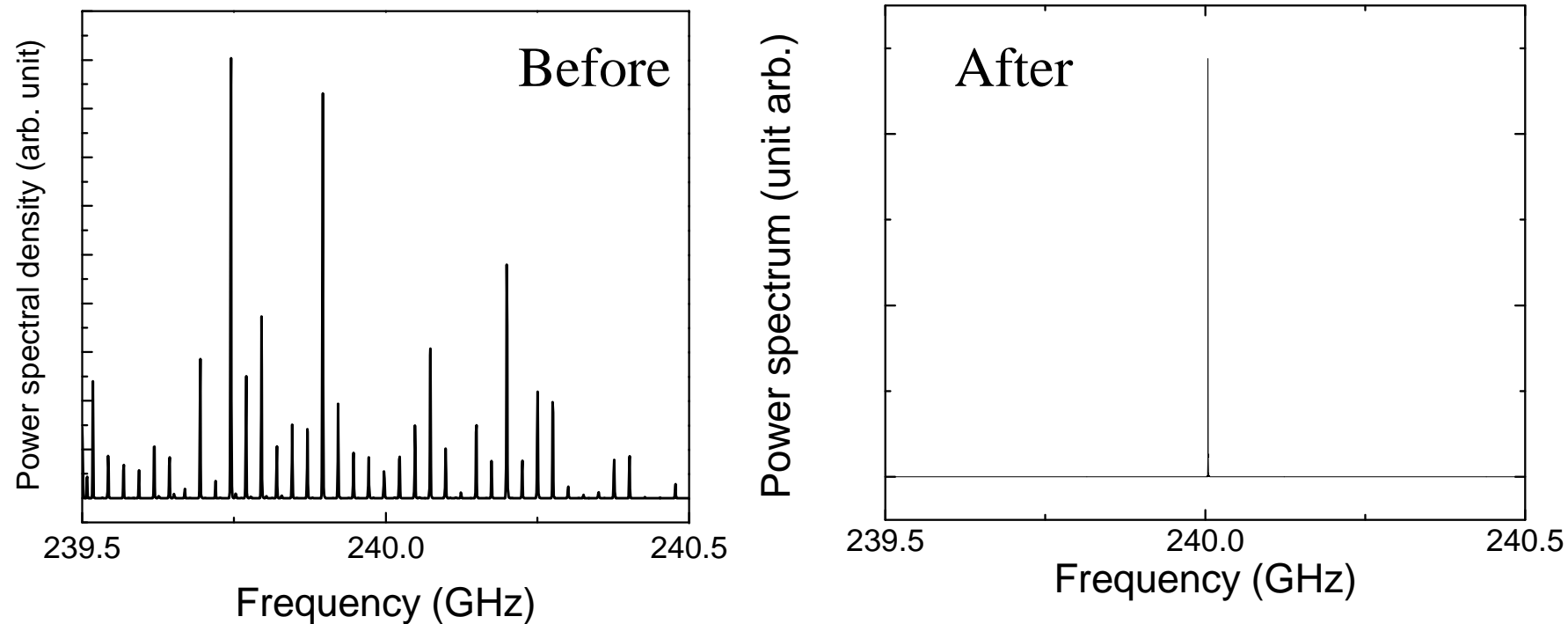


- Two state-of-the-art instruments
 - VDI tunable ultra-stable injection source (~ 30 mW)
 - Thomas-Keating isolator
- Si plate coupler
- 240 GHz spectrum analyzer
- 240 GHz isolator (TK)

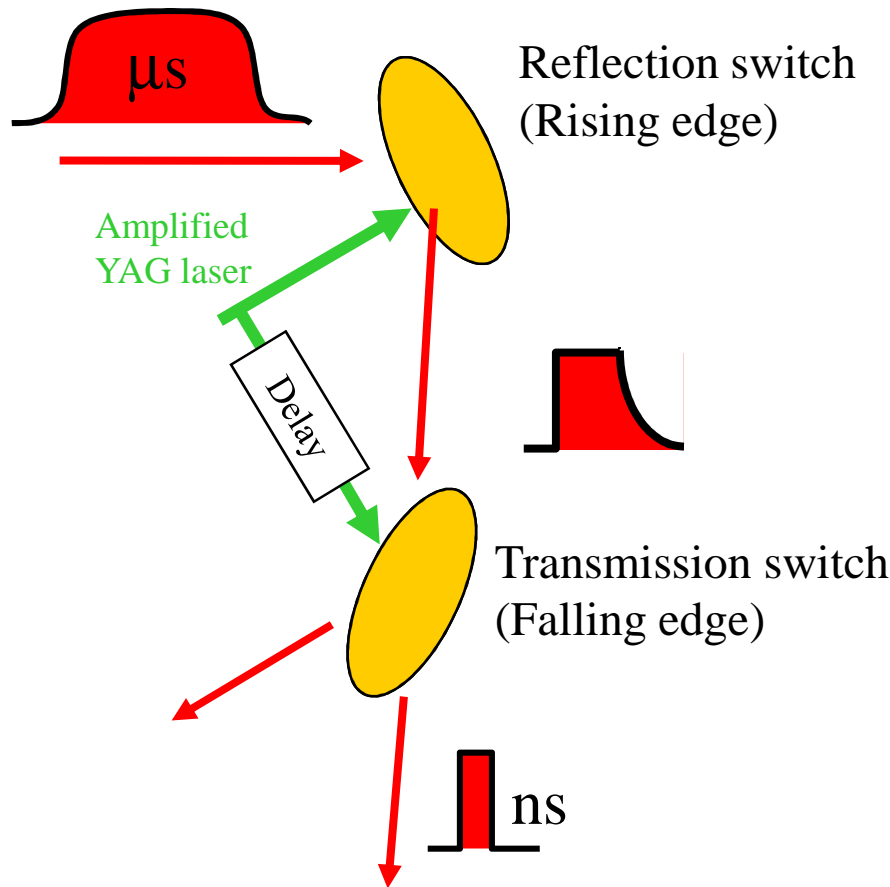


Single-mode lasing

- No pulse-to-pulse frequency fluctuation
- Sub-MHz linewidth (~ 500 kHz@ $2\ \mu\text{s}$ pulse duration)



Pulse slicer

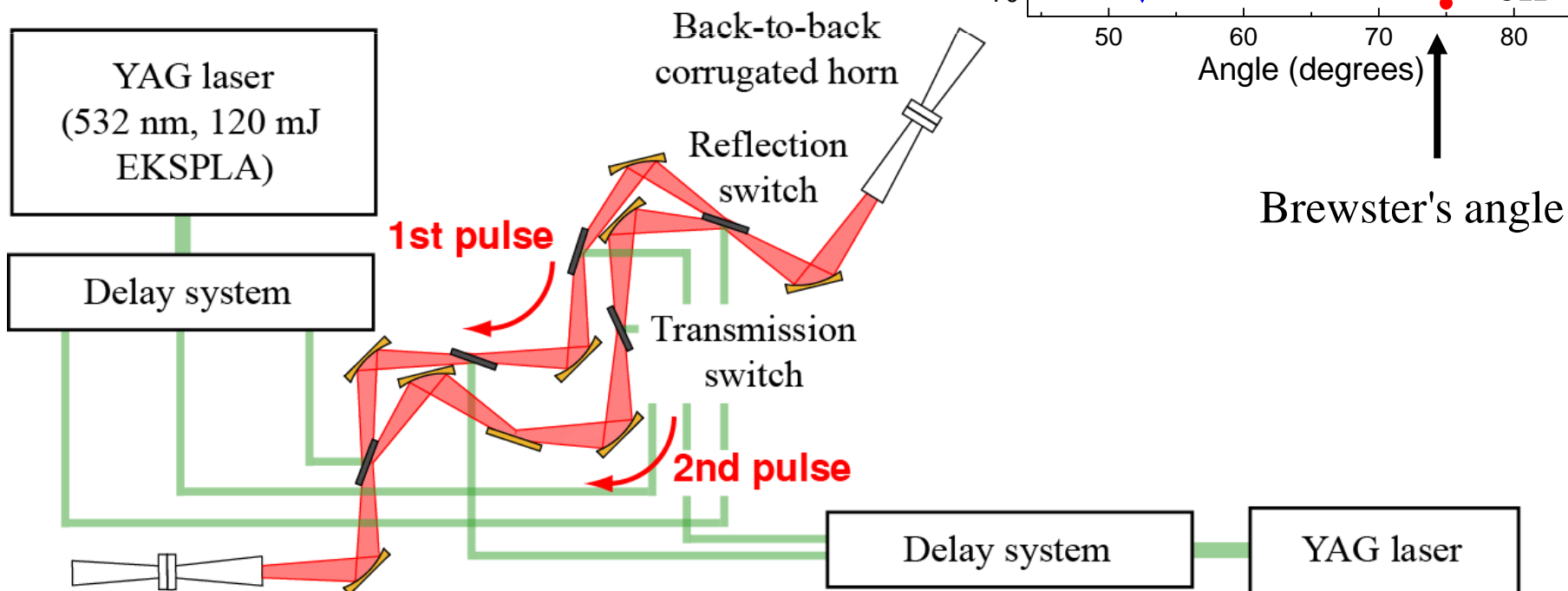


- Pulsewidth is varied by a delay line of YAGlaser.
 - F. A. Hegmann *et al.*, *Appl. Phys. Lett.* **76**, 262 (2000).
 - M. F. Doty *et al.*, *Rev. Sci. Instrum.* **75**, 2921 (2004).
- Pulse slicer is made by photo-activated Si or GaAs switches.
 - Rising and falling times are < 150 ps.

New pulse slicer



- Contrast is a key!
- Tune Si wafer thickness
- > 60 dB contrast ratio



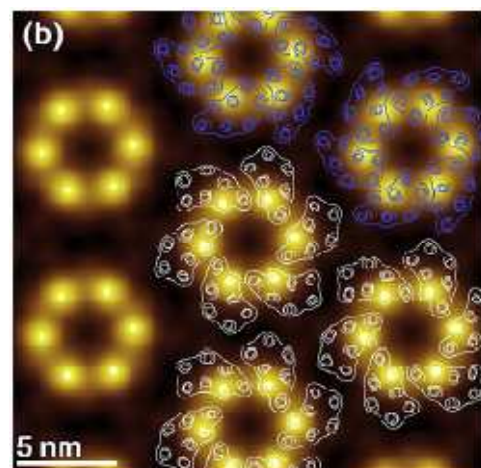
T_2 -based distance measurement



1. Concentration dependence of nitroxide and spin-labeled lipid vesicles



2. DNP of protons.
3. Assembly of proteorhodopsin



proteorhodopsin

A. L. Klyszejko *et al.*, *J. Mol. Biol.* **376**, 35 (2008)



Lipid vesicles in solution

Conclusion

- High-frequency EPR can quench electron spin decoherence with low-temperatures.
- High-frequency EPR can access nuclear spin decoherence.
- FEL-based EPR for ns spin dynamics
- Possible T_2 -based distance measurement

Acknowledgement

- **UCSB - Physics**
 - Jerry Ramian
 - David Enyeart
 - Dan Allen
 - Thor Visher
 - Kiyotaka Akabori
 - Melissa Anholm
 - D. D. Awschalom
- **Delft UT**
 - Ronald Hanson
- **NHMFL**
 - Johan van Tol
- **UCSD**
 - David Hendrickson
 - Chris Beedle
- **UCSB – Chemistry**
 - Songi Han
 - Devin Edwards
- **Research funding**
 - NSF DMR-0321365
 - NSF DMR-0520481
 - W. M. Keck foundation

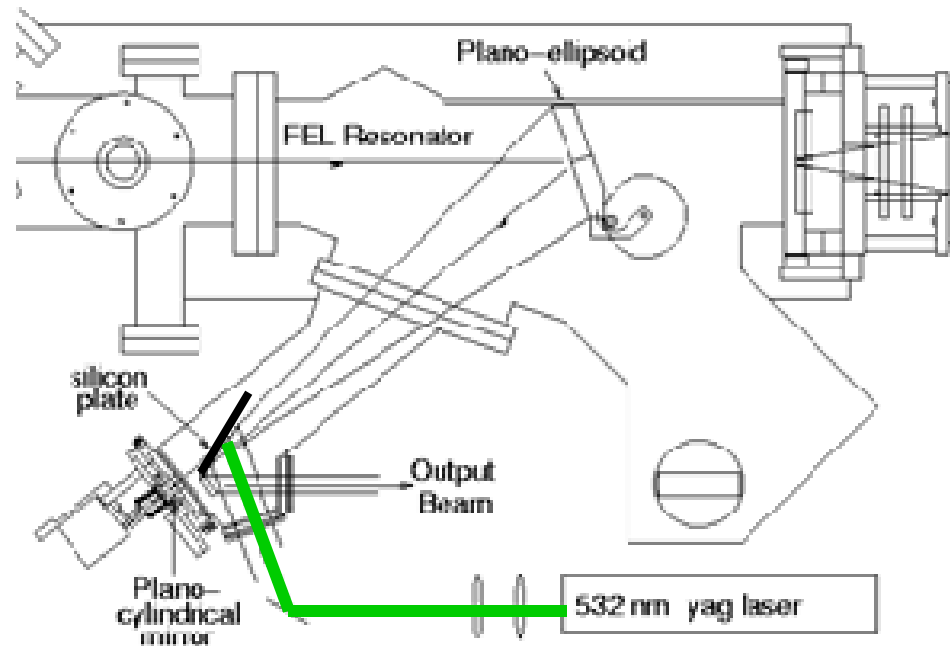


Acknowledgement

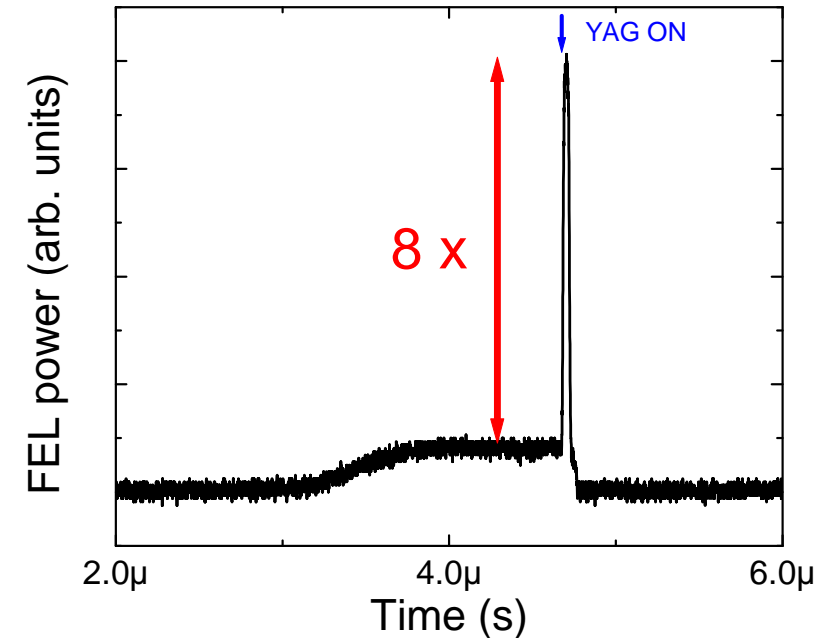


Cavity dump coupler

- Amplification of FEL output for sub-ns time resolution.
- Normal FEL coupler has 5~20 % coupling, so only 5~20 % of intracavity power couples out.
- Cavity dump coupler (CDC) couples out the entire intracavity power.



FEL cavity

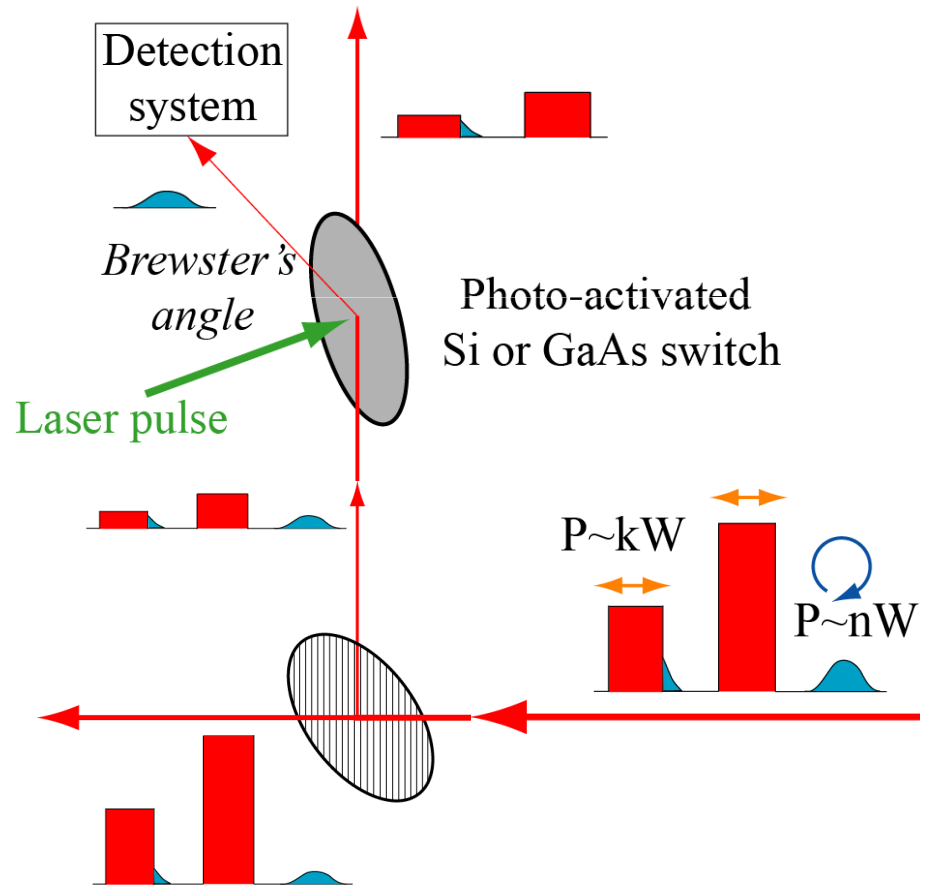


S. Takahashi *et al.*, manuscript in preparation (2009).
J. P. Kaminski *et al.*, *Appl. Phys. Lett.* **57** 2270 (1990)

Isolator

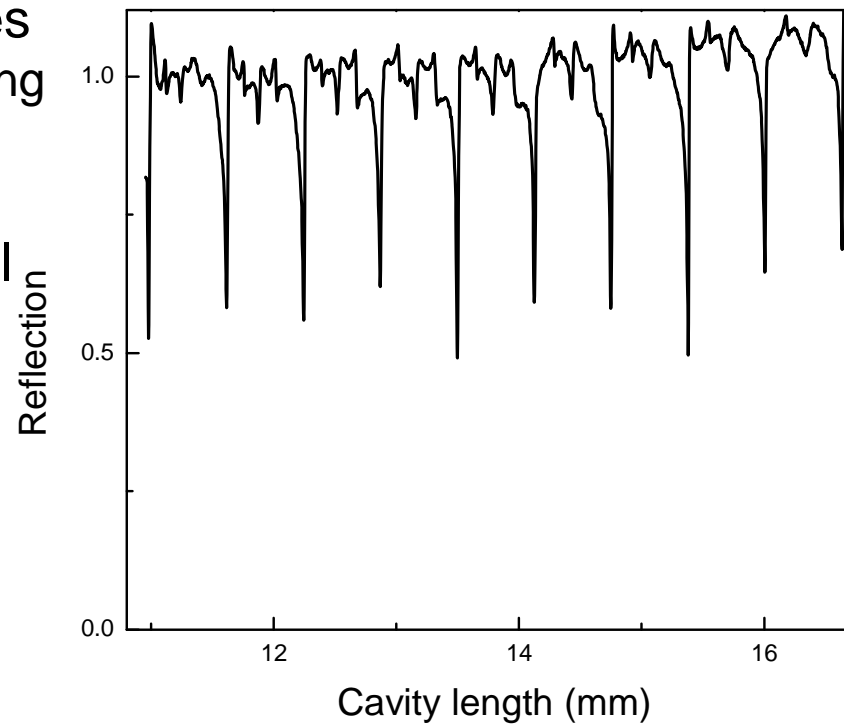
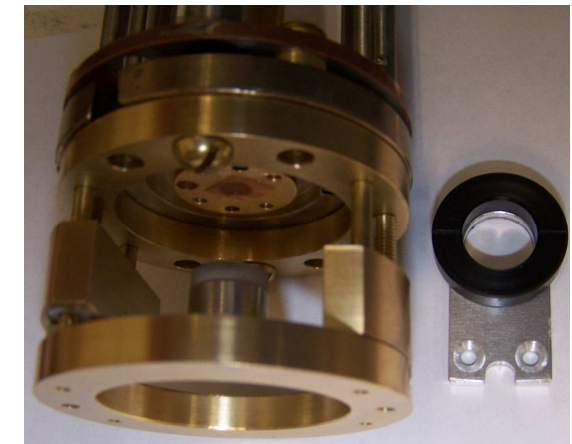


- Huge reflection and tiny sample signal.
- Inputs $\sim \text{kW}$, EPR $< \text{nW}$
 $\rightarrow \Delta P > 120\text{dB}$
- 1st isolation: wire-grid polarizer (EPR is circularly polarized.)
- 2nd isolation: Photo-activated Si or GaAs switch
- Short switching ($< 100 \text{ ps}$)



Fabry-Perot cavity

- Semi-confocal cavity
- EPR couples to H-field; water couples to E-field
- Aqueous sample is mounted at H-field maximum and E-field minimum.
- Two translation stages
 1. End-mirror positioning
 2. Sample positioning
- *In-situ* T-stage control
- Finesse ($\Delta I/I \sim 50$)



“Bottom-up” approach

